Bathymetry, depth to magnetic basement, and sediment Thickness estimates from aerogeophysical data over the Western Weddell Basin

John 1.. LaBrecque[1]
Jet Propulsion Laboratory, Pasadena, California, USA

Marta E. Ghidella
Instituto Antartico Argentino, Buenos Aires, Argentina

Abstract. We estimated the bathymetry and sediment thickness of a remote and difficult to access portion of the Antarctic continental margin using aerogeophysical surveying techniques. 'The U. S., Argentina, Chile aerogeophysical survey collected magnetic and gravity data over the basins surrounding the Antarctic Peninsula. 'f"hir(y-seven of these flight lines were. used to estimate bathymetry and depth to magnetic basement for the western Weddel I Basin. A wave.rlumhcr technique was applied to individual magnetic anomaly profiles in an automated fashion 10 obtain estimates of the depth 10 magnetic basement. The bathymetric estimates were obtained by admittance inversions of the gravity field. The results were then gridded at a 40-km interval for the region 64°W, 44°W, 73°S, and 62°S. Bathymetric estimates and depth to magnetic basement estimates were differenced at each grid point to obtain a regional estimate of the thickness of nonmagnetic overburden (assumed to be sediment). Subsequent spot measurements of topography in the estimated region of the continental margin gc[lc.rail y agree 10 about 52 meters. The estimated magnetic base.mcn[deepens from the Antarctic-Peninsula margin eastward to a maximum of 10-12 km near 54°W. We also postulate the existence of two moderately large basins flanking the eastward continuation of the Jason Peninsula. Farther east, the basement steps upward, with a correspondent thinning of the sedimentary layer. Along the east coast of the peninsula, results agree. well with seismic. studies on James Ross Island and magnetotelluric studies on Marambio Island and the Larsen nunatak, as well as the British Antarctic Survey basement estimates from acromagnetic data. This study further demonstrates the utility of combined application of airborne and satellite. geophysical techniques in the study of structure and tectonic evolution of continental margins and marine basins.

Introduction

The basins surrounding the Antarctic Peninsula compose one of the most inaccessible regions of Earth. Heavy year roundice cover and frequent and severe storms combine to make exploration of this region extremely difficult and lime consuming. Consequently, bathymetric maps of the region arc based on very limited data. A great deal of interpretation base.d on the geologic intuition of the cartographer is required to turn this sparse data set into a regional map. This uncertainty in the structure and location of the continent margins is problematic from the viewpoint of basin circulation studies, plate tectonic reconstructions, regional rifting models, and exploration planning. The U. S., Argentina, Chile (USAC) program conducted an extensive aerogeophysical survey (Figure 1) to determine the structure and development of the continental margins and basins adjoining the Antarctic Peninsula and southern South America, The USAC flights employed a long -

range 1'-3 Orion provided by the U.S. Naval Research Laboratory Detachment at Patuxent River Naval Air Station, Maryland. The aircraft was equipped with a gravimeter, proton precession magnetometer, as well as Global Positioning System (GPS), Omega, and inertial navigation systems. GPS navigation now permits the usc of long-range aircraft without local navigation networks which significantly improves the effectiveness of aerosurveys over remote regions. Aerogravity technology has been described by *Brozena* [*1984*] and by *Brozena and Peters* [*1988*]. USAC successfully carried out the first operational lorrg-range aerogravity survey and the first such sur vey over an ice-covered continental margin [*Brozena et al.*, 1987].

The gr avity and magnetic data sets arc our best source of information concerning the regional structure. Figure 2 shows that pr ior to the USAC survey there were fcw geophysical data fur the Antarctic Peninsula margins. The data collected by the long-range P-3 Orion complement existing data sets such as the compilation of the available gravity, magnetic, and seismic data for the circum-Peninsula basins of the Ocean Margin Drilling (OMD) Region 13 Atlas [*LaBrecque et al.*, *1986*] as well as the aeromagnetic surveys of Britain [*Renner et al.*, 1985] and the former Soviet Union [*Maslov*, 1980] which have gathered aeromagnetic data over nonmarine portions of West Antarctica.

We combined USAC aerogravity [*Brozena et al.*, 1987] and Geosat gravity [*Haxby*, 1988; *Haxby and Hayes*, 1991; *Marks and McAdoo*, *1992*] data sets to increase the coverage of the western Weddell Basin (Plate la), although gaps still remain in the gravity coverage. in a similar manner we developed a gridded magnetic anomaly field using the USAC and other available databases as shown *in* Plate lb. *Bell et al.* [*1 990*] suggested that the strong linear north-south striking gravity gradient along the eastern margin of the Antarctic Peninsula in Plate 1 a could cor respond to the. shelf edge. This imp] ies significant bathymetric errors in compilation of General Bathymetric Chart of the Oceans (GEBCO) map 5:16 [*Johnson et al.*, *1983*] as well as most of the digital bathymetric data sets of the region which arc derived from this car log, aphy.

The western margin of the Weddell Basin developed in Middle to Late Jurassic time as evidenced by the seafloor spreading pattern [*LaBrecque and Barker*, *1981*; *LaBrecque et al.*, 1986] (Figure 3) and the observation of Jurassic shallow water marine sediments on the western Weddell margin, the. Falkland Plateau [*Ludwig et al.*, 1980], and the Magallanes Basin [*Natland et al.*, 1974]. The Jurassic and younger sedimentary accumulation on the western margin of the, Weddell has been termed the Larsen Basin [*Macdonald et al.*, 1988] and is considered to have significant hydrocarbon potential [*St. John*, 1986; *Behrendt*, 1990]. The Larsen sedimentary sequence is floored by the Jurassic Nordenskjold Formation and extends through to the mid-Tertiary with an apparent hiatus or unconformity in the. Early Cretaceous [*Rinaldi*, *1982*; *Farquharson*, 1982, 1983; *del Valle and Fourcade*, 1986; *Olivero et al.*, 1986; *Elliot*, 1988; *Whitham and Storey*, *1989*] which is dominated by alternating radiolar i an rich mudstones and ash beds laid down in euxinic conditions. In this study wc used the USAC aerogeophysical

data set to determine the bathymetry of the western Weddell margin and sedimentary thickness of the Larsen Basin and the western Weddell Basin.

Revision of the Regional Bathymetry

One method of estimating bathymetry in an uncharted region is to determine the relationship between gravity rrnd bathymetry or the admittance function in a nearby region where both the gravity and bathymetry have been mapped and then apply that admittance function to the unknown region. *Dorman and Lewis [1970], Lewis and Dorman [1970]* and *McKenzie and Bowin [1976]* have shown that the relationship between gravity and bathymetry can be approximated by a linear function of the form

$$G(k) = Z(k)B(k) \quad (1)$$

where

$G(k)$	Fourier transform of the free air gravity anomaly;
z(k)	admittance func Lion;
$B(k)$	Fourier transform of the bathymetry;
k	wavenumber.

When the bathymetric relief is small and varies about an average depth, $Z(k)$ is real and independent of $B(k)$. The admittance function has been used to study the mechanism of isostatic compensation and the elastic properties of the lithosphere [*Walcott, 1970, 1972; Steckler and Watts*, 1978; *Watts and Daly, 1981*].

An estimate of bathymetry can be determined by solving for $B(k)$ given an estimate of $Z(k)$ derive.d from an area where both $G(k)$ and $B(k)$ are known. The admittance function may vary considerably from onc location to another and can be difficult 10 estimate accurately.

Variations are induced by differences in the geologic structure and geologic history from one region to another. For example, a passive continental margin which is morphologically uniform along its extent can exhibit a variation in the admittance function along strike if the isostatic response to sediment loading varies along the margin. A difference in isostatic response along the margin could develop if a major influx in sedimentation occurred in onc region when the lithosphere was relatively Lhin and weak while at another location major sedimentation occurred several million years later over stronger and thicker lithosphere. For this reason we must determine the admittance function from regions which share a common evolution. Measurement noise, particularly in the gravity database, will also contribute Lo errors in $Z(k)$.

Most importantly, the strong relief of a continental slope and the usc of a discrete Fourier transform result in an ill-behaved and "spiky" complex admittance function in contrast to the smooth linear and real thrmrc.tics] admittance. function for smoothly varying low relic.f topography. *Karner and Watts [1982]* reduced the effect of the pole.s and m.roes in the individual admittance spectra by averaging several profiles from regions with varying widths of the continental slope using

$$Z(k) = \frac{\sum_{n=1}^{N} G_n(k) B_n^*(k)}{\sum_{n=1}^{N} B_n(k) B_n^*(k)} \qquad (2.)$$

where N is number of profiles averaged in the ensemble and the asterisk signifies the complex conjugate.

Following this technique, we selected as a reference area the northwestern Weddell Basin where bathymetry has been relatively well measured by satellite-navigat e.d icebreakers [*Keller et* al., 1985]. Opening models by *Labrecque et al. [1986]* and *Grunow et al.* [1987] suggest that the western Weddell margin evolved in a uniform manner from north to south. Five profiles were extracted from the gridded gravity and bathymetry of this reference area within the latitude bounds of 65°S and 66°S. An average of the admittance function was estimated from the five profiles. This estimate of $Z(k)$ was then applied 10 the length of the western Weddell Basin using the combined acrogravity and Geosat measurements. The.rc.sulling bathymetric estimate proved less than satisfactory and belied our notions of realistic shelf structure because long-wavelength gravity components were amplified by the admittance function into large basinlike structures on the continental shelf.

In Figure 4 we compare Lhc observed admittance from our reference section (o the theoretical linear mode.t for various elastic thicknesses. The observed admittance function averaged from five reference profiles exhibits much higher variability in amplitude than the models which arc dc.rived for lithosphere at mean waler depths of 2..5 and 10 km. A theoretical admittance function derived for a mean water depth of 10 km ar id an elastic thickness of 40 km appear to match the observed admittance best. Although an elastic thickness of 40 km for the Jurassic margin is reasonable, this match is highly suspect given the steplike nature of continental margin and the fact that the scdilnclll-water interface is nowhere greater than 5 km near thcwc.stern Weddell margin.

The necessar y conditions for the linearity of the admittance function arc not well satisfied at continental margins. The Weddell margin topography can be approximated by a step function, with an amplitude of 4 km. The large asymmetric relief of the continental slope induces nonlinear effects in the gravity field. *Karner and Watts* [1982] suggested that nonlinear effects at a continental margin should cancel out when averaging is performed over several profiles with different slopes; however, they used a linear gravity model to derive the admittance relationship.

If a nonlinear approach to modeling the anomaly field is used, the admittance function for the synthetic margin (the appendix) has a nonzero phase whose asymptotic behavior is controlled by (he. factor $e^{i(kT-\alpha)}/\sin(kT)$, where k is the wavenumber, T is the half width of the continental slope, and α is the angular complement of the continental slope and is slightly smaller than $\pi/2$. The $\sin(kT)$ factor limits the phase angle to absol ute val ues less than $\pi/2$ (Figure Al) and induces π discontinuities al kT values which arc integer multiples of π, except for k= O, where the phase tends to zero. If the π discontinuities are removed (which is equivalent to changes of sign in the. admittance function for sectors for which

$m\pi < kT < (m+1)\pi$, with m odd), then the resulting phase will be a straight line with slope equal to kT for large wavenumbers. A linear fit to the phase slope will provide an estiumate of the average. width of the continental slope. Variations in the phase of the admittance function will also be induced by incomplete compensation of the surface topography. Averaging several profiles with different slopes and local isostatic compensation will reduce the phase excursions, but the slope in admittance phase will remain. A shift in the true position of topography with respect to expected topography will also induce a linear phase shift.

If the Fourier transforms of gravity and bathymetry arc linearly related, then the phase of the admittance function is zero. However, the phase of the observed admittance functions in Figure 5 vary strongly with both 2π and π discontinuities. The 2π discontinuities arc easily explained, but the π discontinuities arc more problematic. If wc remove the π and 2π discontinuities, then we observe line.ar trends which arc related to the continental slope as discussed above.

Figure 5a is one of the profiles used [0 calculate the reference admittance (latitude 65050), and Figure 5b is a more southern profile at latitude 68°40' where the GEBCO topogr aphy is suspect. The plot at the left top of each figure shows the unwrapped phase, which is the spectral phase obtained when 2π as well as π discontinuities arc removed from the $+/-\pi$ bounded phase (left, middle). Two linear least squares fits WCIC made to the.sc curves: onc from $k = 0$ to $k = 0.05$ km^{-1} that is for relatively low wavenumbers, and the other from $k = 0.05$ km^{-1} to $k = 0.2$ km^{-1}. The corresponding slope values are written on the plots. Figure 5b has a much steeper slope for the unwrapped phase, which indicates a difference in the relative position of gravity and bathymetry of about 128 km between the two profiles. Also note that the amplitude spectra both strongly vary and do not decay with wavenumber.

In order to better understand the departures between our observed admittance and that of the the.orc.tical admittance functions, wc examined the analytical expression for the admittance of an unsedimented continental margin in Airy isostatic compensation. The details arc explained in the appendix.

The linear admittance model and the studies of *Karner and Watts* [1982] suggest that the amplitude of the admittance function should decay for large wavenumbers, while both the analytic results (in the appendix) and our single profile admittance functions indicate that the admitttance amplitude does not decay with increasing wavenumber. The decay in Figure 4a suggests that the avc.rage depth of the margin should bc 10 km yet this would require that half of the. basin is below 20 km, which is over 3 times deeper than most old ocean basins. The amplitude of the analytical admittance for the compensated synthetic margin behaves like the linear admittance function for low wavenumbers. At intermediate and lar ge wavenumbers the admittance has poles at the zeros of $\sin(kT)$ (Figure A 1) and does not diminish in amplitude.

Destructive interference in the averaging process might smooth the amplitude spectrum of the admittance; however, the limited number of independent profiles available. to us was not sufficient to nullify the effect of poles and zeroes i n

amplitude spectrum (Figure 5a). A comparison of admittance functions derived from individual and averaged profiles indicated that the admittance smoothing was small and sonic.linlcs unnoticeable.. Wc also found that observe.d admittance has minima in addition to the maxima as shown in Figure Al. Our experimental modeling indicated that these minima can result from an imperfect isostatic compensation. When compensation is exact, the gravity and topography extrema arc coincident which smoothes the amplitude spectrum of the admittance (Figure Al).

The inver sion of equation (1) 10 solve for the bathymetry is difficult even in cases where the linear approach holds nicely because the admittance tends to zero for low wavenumbers whose energy dominates the spectrum of continental margins. The oscillatory nature of the admittance amplitude makes the inversion even more difficult. Finally, wc have shown that in the Fourier domain, gravity is a nonlinear function of bathymetry over continental margins.

The admittance still contains significant information on the shape of the bathymetry and its compensation. The admittance phase appears to retain considerable information o n the relative position of the topography and gravity structure at the shelf break as well as information on the shelf Slope..

Given the apparent robustness of the admittance phase estimates compared to the admittance amplitude estimates, w c attempted a second technique as suggested by G.D.Karner. We calculated the admittance functions for several gravity and bathymetr ic pro files in the southern sector and substituted the phase component from the northern reference admittance. This is approximately equivalent 10 repositioning the topographic structure of a selected profile according to the relationship of gr avity and bathymetry in the reference profile. The method can be summarized as follows.

1 f the reference admittance is

$$Z_r(k) = A_r(k)e^{i\theta_r(k)} \tag{3}$$

and the admittance of the profile to be adjusted is

$$Z_s(k) = A_s(k)e^{i\theta_s(k)}, \tag{4}$$

then the new admittance of the adjusted profile is

$$Z_n(k) = A_s(k)e^{i\theta_r(k)} \tag{5}$$

and the new adjusted topography is

$$B_n(k) = \frac{G_s(k)}{Z_n(k)} = B_s(k)e^{i[\theta_s(k) - \theta_r(k)]}. \tag{6}$$

We applied the correction of equation (6) to 21 profiles in a 350 km latitudinal band from 66°S LO 69.5°S. Because of sparse (three profiles) gravity coverage (Plate 1a) and the apparent curvature of the margin wc did not extend our inversion farther south. Instead, wc interpolated the bathymetry from 70°S to its intersection with the southern

continental slope near 72°S and 53°W which is a better explored region. The estimation of bathymetry along, the margin south of 69.5° S and west of 53°W was done by assigning a bathymetric value of 500 m 10 10 points along, the gravity maximum and regridding the bathymetry using the eastern GEBCO bathymetry and the western revised bathymetry in the area described above.

Plate 2 displays the newly estimated bathymetry as a contoured color image. The GEBCO bath ymetry is shown as red dashed thousand-meter contours. If the structure and gravity/topography relation is the same as for the northern Weddell margin, then the shelf edge is located along the gravity maximum and the GEBCO shelf edge for the western Weddell Basin is in error by as much as 100 km eastward along the southwestern margin of the basin. At the time of th is writing, the *AnZone* [1989] program (which was provided with our revised bathymetry) began to return bathymetric data from a drifting ice station and helicopter stations along the continental slope of the western Weddell [*Gordon et al.*, 1993a,b]. The results arc in excellent agreement with our bathymetric predictions. of 127 soundings distributed over the region, the mean difference between predicted and observed topography averaged less than 80 m with a standard deviation of 5'2 m. A maximum error occurred at 70.3°S and 55°W, where the gravity field displays a strong negative seaward gradient. The estimated topography was 2406 m, while the. measured depth is 1130 m, suggesting a very steep continental slope 10 the east of this point.

Depth to Magnetic Basement

Figure 6 displays the tectonic interpretation of the magnetic anomaly field for the western Weddell shown in Plate 1a. The tectonic pattern has been derived from previous studies [*LaBrecque and Barker*, 1981; *LaBrecque et al., 1986,* 1989] and has been extended using the USAC magnetic anomaly database. Generally, the magnetic anomaly pattern is subdued with anomalies rarely exceeding 50 nT in amplitude. Strong magnetic anomalies arc located over the Antarctic Peninsula and the Bransfield Straits as well as the Orion Anomaly (named after the }'-3 Orion aircraft which mapped the anomaly) in the southern Weddell. The source of the. orion Anomaly is likely a volcanic pile at the. ocean-continent boundary of the souther n margin of the Weddell Basin.

Lineaments of magnetic anomalies strike northeast and northwest in the deeper portions of the basin. The northeasterly anomalies have been interpreted as the traces of fracture Y.ones, while the northwesterly anomalies a•:·' lilt. conjugate seafloor spreading magnetic anomalies [*LaBrecque et al., 1986,* 1989]. The oldest crust in the Weddell Basin is likely Jurassic in age. and borders the continental margins. The crust becomes younger to the north and east, reaching Oligocene age at the Endurance Collision zone. During the evolution of the western Weddell Basin the seafloor spreading direction has changed nearly 90° with respect 10 the peninsula, resulting in a large age contrast at a shear zone near 65°S and 47°W. Evidence for this shear zone lies in the

interpretation of the magnetic anomaly pattern of seafloor spreading anomalies within the basin.

We have attempted to derive crustal structure from depth to magnetic basement estimates. We used individual flight lines because although the USAC flight line density of 36 km is adequate for regional anomaly identification, the analysis of a gridded database for depth to magnetic source requires nearly an order of magnitude greater data density.

The profile.s were analyzed assuming that the. distribution of source.s is constant perpendicular to the flight path. This assumption of two-dimensionality in the source distribution]] might introduce some bias toward deeper magnetic basement estimates. *Shure and Parker* [1981] have shown that linear sampling of a three-dimensional magnetization distribution can introduce the spurious amplification of long-wavelength spectral components through strike aliasing. In depth to basement measurements this will produce erroneous deeper basement estimates. Most profiles in the USAC aerosurvey were flown m thogonal to regional trends (northwest or northeast) in the magnetic anomaly pattern; therefore we expect that this effect will be minimized in the. average..

W C . investigated several methods of estimating depth t o magnetic base.mcnl including statistically based spectral estimations as described by *Spector and Grant* [1 970] and *Treitel et al.* [1971] and high-resolution techniques such as Werner deconvolution [*Hartman et al.,* 1971], analytic signal analysis [*Nabighian,* 197'2], and the composite method of Phillips [1975]. Automated analysis was deemed necessary 10 process the large amount of data involved and to minimize the potential of bias in interpretation.

The most successful technique was a variation of the. spectral analysis method. The technique assumes that magnetic basement is composed of a randomly distributed layer of magnetic source.s of thickness T at a depth d M o w the level of observation. The magnetization is assumed constant in dire.ctioll but variable in intensity. The Fourier transform of the resultant anomaly field [*Schouten and McCamy,* 1972] is

$$F(k) = 2\pi CM(k)e^{-kd}(1 - e^{-kT})e^{-i\theta} \qquad (7)$$

where

k scalar wavenumber;
a' depth to the top of the source layer;
M (k) Fourier transform o f the magnetization distribution;
C amplitude term which is a function of the magnetization and ambient field directions;
*''f thickness of the magnetized layer;
O phase term, function of ambient and remnant field directions relative to the strike of two-dimensional bod y.

The power spectrum of $F(k)$ is

$$S(k) = Ae^{-2kd}(1 - e^{-kT})^2 \qquad (8)$$

WI ICI e A is a constant. If $T>>d$, then

$$ln[.\$(k)] = -hi(A) - 2kd. \qquad (9)$$

Wc see from (9) that the log power spectrum of the anomaly field falls off as a line.ar function of wavenumber. Estimates of depth to source Lhc.rc.fore can be made by a least squares fit of (9) to the power spectrum of the anomaly profile. As in all inversion schemes, several practical considerations will introduce errors. First, the shorter wavelengths may contain measurement noise such as ambient field fluctuations, instrument, and navigation noise. Second, the assumption that the thickness of the magnetic source is greater than depth may not always hold, such as over oceanic crust where estimates of magnetic source thickness vary from 5 to 0.5 km, while the depth to source may vary between 2.5 km and 7 km. Last, departures from tbc assumption of two-dimensional sources will increase the depth estimates.

The linear fit of (9) [o the observed log power spectrum is can ied out in a band between wavenumbers $k_l < k < k_u$. k_l *is* set to 0.018, a wavelength of 333 km, while k_u is defined by estimating the mean noise level and its standard error at short wavelengths. k_u is located at tbc intersection between the power spectrum at longer wavelengths and tbc upper limit of the estimation band which is the mean power plus twice the standard er ror at the noise floor. Estimates were rnadc from a 250 km moving window. The window overlapped at 10-km intervals. Therefore the same point along the profile is "visible" for 25 estimates of depth. After removing the linear trend and mean value., zeroes were appended to the windowed data for a total spectral length of 1024.

Wc found that the stability in the depth estimates was improved by estimating a source. thickness. A value. of T= 2 km was used for the source. thickness in accordance with the approximate thickness of oceanic layer 2. We tested the technique on a synthetic profile generated by sources of varying depth and source thicknesses. The depth [o source. was varied in a sequence of steps from 5 km to 1 km. The estimates of source depth for the synthetic profiles were accurate. to about ?.0% in the absence of measurement noise.

The spectral technique was applied to over 180,000 km of flight lines. Estimates of depth to magnetic basement were obtained at IO-km intervals along these flight lines. The region was covered with approximately four depth estimates per thousand square kilometers. The depth estimates were corrected for aircraft altitude and averaged within a 40-krn grid interval. One check on the accuracy of the gridded estimates was to compare the estimated source depth in the Drake Passage where seismic data and well identified seafloor spreading anomalies permit a reliable. identification of the magnetic source depth of between 4 and 5 km below sea level. our estimated source depths in tbc Drake Passage were within 20% of these values. The rc.suits of our method also compared very well (< 1km) with the Werner clc.convolution estimates for the Bransfield region of *Parra and Yanez [1988],* who used a combine.ci USAC and Chilean aerosurvey data set [*Parra et al.*, 1984] to estimate depth to magnetic basement.

Figure 7 displays a contour map of tbc depth to magnetic basement. Basement generally dips eastward from the. shoreline of the Antarctic Peninsula with a rapid increase in depth which avc.rages 9-14 km along, a southwest trending trough whose northern terminus is al 64°S, 51°W. This

trough lies well west of the shelf edge as mapped by GEBCO, which could indicate either a major sedimentary basin within the margin or, as wc believe, an error in the GEBCO bathymetry. The magnetic basement map indicates a shoaling of basement which trends southeast from the Jason Peninsula which divides the western shelf into two basins. Wc have named the structure, the Jason Horst.

l'late 2 indicates the presence of bathymetric depressions over the. northern and southern subbasins. Over the oceanic crust (refer to l'late. 2) the basement tends to shoal as the crust becomes younger. Note that near the shear zone of the northwestern Weddell Basin, the basement is deep (10-11 km) over the Jurassic crust and shallower (< 9 km) over the Cretaceous and younger [tot to the east of the shear zone. The nmrc shallow crust is still quite deep for the youngest crust which should bc Oligocene to Eocene age, although sediment accumulations may be depressing the crust in this area. This crustal shoaling is also coincident with a strong gravity gradient in the Geosat gravity field (Plate 1a) and strong, gradients in the magnetic field (Plate lb).

Regional Sediment Thickness Map

in the final step we subtracted the revised bathymetry from the depth to magnetic basement in order to estimate the. thickness of the nonmagnetic overburden. 10 order 10 discriminate between sediment thickness as estimated by seismic and drilling results and the usc of modified depth to basement estimates in this work u'twill refer to thickness of nonmagnetic overburden (Nell) as our estimates of sediment thickness.

The thickness of nonmagnetic overburden (Plate 3) increases from approximately 3-4 km at the eastern shoreline of the Antarctic Peninsula (similar to the estimates of *Renner et al.*. [1985] to about 4-6 km at the edge of the shelf. Seaward of the shelf edge the nonmagnetic overburden increases dramatically to 8-12 km. *LaBrecque et al.* [1989] considered this region to be the silt. of earliest rifling in the. Weddell Basin during the Middle. Jurassic. The eastward increase in nonmagnetic overburden is also observed by the only seismic results recorded in the eastern Peninsula by *Keller et al.* [1989], who reported a 4° eastward slope in the Mesozoic and younger sediments on James Ross island and sediment thickness on the order of 4-5 km. Magnetotelluric experiments [*del Vane et al.*, 1988] report a 6.7-km sediment layer on Seymour Island, in fair agreement with our estimates. The study also presents results over the Robertson island region (near 65°S, 59.5°W), where they find an anticline in the basement flanked by sediments up to 4 km thick.

The nonmagnetic overburden shown in Figure 8 indicates a 2-km change in NOB thickness which correlates to a 2-km change in depth to basement across the paleoshear zone. The abrupt age contrast and the resulting bathymetric relic.f predicted from this age offset likely generated a barrier to eastward sediment transport and ponded sediment west of the shear zone. *Grikurov et al. [1990]* gathered a multichannel seismic profile across this portion of the margin and the proposed shear zone, and they report sediment thicknesses

which correspond to our NOB estimates. *Kavoun and Vinnikovkaya* [1994] compiled a depth to acoustic basement map of the. northwestern Weddell from seismic measurements of the R/V Geolog Nalivkin. The compilation generally agrees with that presented in this study dc.spite the difference in techniques and resolution. Acoustic basement might gene.rally be expected to lie above magnetic basement in studies of this sort. The map of acoustic basement also shows a 2 to 3 km westward deepening in acoustic basement across the proposed paleo shear zone between 64°S to 65°S along the 312°E meridian.

lhc.N(Hlrc.sobs also locate several basins along the shelf edge which should bcof Jurassic age. The basins arc generally locale.d in areas between the intersection of southwest-northeast striking magnetic anomalies which wc have interpreted to be fracture zone trends and the shelf edge.. in the. southwestern portion of the region (near 71°S and 60°W), wc observe a broad deepening of magnetic base.mc.]11 and a consequent thickening of nonmagnetic overburden in the southwestern Weddell Basin near 70°S and 60°W. This may be a northward continuation of the 10-kn]-deep basin [*Kadmina et al.*, 1983] which extends northward beneath the Ronne Ic c. Shelf. *Maslanyj and Storey* [1990] also report basement depths of the order of 10-12 km surrounding the Haag Nunataks at the base of the Antarctic Peninsula.

1 arsen Rift

González-Ferrán [1983] has suggested the existence of the Larsen Rift in the region of the James Ross island based upon the observation of recent surface volcanism. We have not observed magnetic anomaly patterns or significant magnetic anomalies in the region of the proposed Larsen Rift. Our solutions of depth to basement in the region show no significant change in depth to magnetic basement. Such anomalies would be expected from accumulations of volcanic material or major disruptions in basement. The absence of such magnetic anomalies arc not sufficient in themselves 10 disprove the existence of the Larsen Rift. However, they do indicate that if the rifling is presently active, then volcanic activity is in a very nascent stage.

Conclusion

The acrogravity and acromagnetic data gathered by the USAC acrosurvey over the western Weddell Basin and the available Geosat gravity field have been combined slid analyzed to produce bathymetric, depth to basement, and estimated sediment thickness estimates for a difficult to access region of die. Antarctic margin. We have shown that the phase. information from an averaged admittance function can be used to derive bathymetric estimates from the gravity anomaly field at passive continental margins. Location of the shelf edge in the western Weddell Basin has been relocated as much as 100 km west of the location mapped in the GEBCO map series. The integrated analysis of revised bathymetry and the depth to magnetic basement indicate an eastward thickening of the sediment overburden in the western Weddell Basin and a major

accumulation of sediment at the shelf edge. This study demonstrates the utility of long-range aerogeophysical surveying in remote areas.

APPENDIX A: Analytic Expressions for Admittance of Continental Margins

In the following, we derive the analytic expression for the gravity field and admittance of a simple continental margin which transforms from shallow water to oceanic depth w along a linear continental slope whose width is 27'. The Fourier transform of the gravity anomaly due to the bathymetric interface of this model is

$$G_s(k) = -\frac{2\pi i G(\rho_w - \rho_c)}{k^2}\cos(\alpha)e^{-i\alpha}[e^{ikT} - e^{ikT}e^{-kw}] \quad \text{(A1)}$$

where

- k wavenumber;
- G universal gravity constant;
- ρ_w water density;
- ρ_c crust density;
- α angle between the continental slope and the vertical such that

$$\tan(\alpha) = \frac{2T}{w} \quad \text{(A2)}$$

Adding the contribution of the mantle assuming Airy isostatic compensation we obtain the Fourier transform of the total gravity anomaly over the model continental margin

$$G_p(k) = -\frac{2\pi i G(\rho_c - \rho_m)}{k^2}\cos(\beta) \cdot e^{i\beta}e^{-k(w+t)}[e^{ikT} - e^{ikT}e^{-ikT}] \quad \text{(A3)}$$

where

- w' Upper bound of the Moho relief corresponding to an ocean depth W;
- t oceanic crust thickness assuming local mass compensation at depth T_c, the base of the continental crust;
- ρ_m mantle density;
- β angle between the mantle slope and the vertical determined by

$$\tan(\beta) = \frac{2T}{w'}. \quad \text{(A4)}$$

Following *Karner and Watts [1982]*, the bathymetry is defined as the scaled convolution of a signum function and a rectangular window of width T so that

$$B(x) = -\frac{d}{2T}sgn(x) * \text{win(x)} \quad \text{(A5)}$$

where the asterisk signifies convolution, x is the coordinate along the profile, and d is the median water depth. The Fourier transform of the bathymetry is then

$$B(k) = -\frac{2id\sin(kT)}{k^2T}. \quad \text{(A6)}$$

We can now write the equations for the admittance

$$Z(k) = \frac{G(k)}{B(k)} = \frac{G_s(k) + G_p(k)}{B(k)}$$

$$= \frac{\pi G T}{d \sin(kT)} [(\rho_c - \rho_w)\cos(\alpha)e^{-i\alpha}(e^{ikT} - e^{-ikT}e^{-kw})$$

$$+ (\rho_m - \rho_c)\cos(\beta)e^{i\beta}e^{-k(w+t)}(e^{ikT}e^{-kw'} - e^{-ikT})]$$

. (A7)

$Z(k)$ in (A7) decreases smoothly 10 zero for low wave.numbers, a necessary condition for this being the exact compensation of the topography. For very large wave.murnbcrs (short wavelengths) or deep compensation depths, $G_p(k)$ or the gravity effect of compensation vanishes, and the spectrum of the admittance is controlled by the factor $e^{i(kT-\alpha)}/\sin(kT)$ which is the effect of the surface topography. The term $\sin(kT)$ with its zeroes al $kT = m\pi$, m being an integer, limits the absolute value. of the phase to less than $\pi/2$. Note that α (equation (A2)) is a little smaller than n/2, with typical values of w and T being 4 km and 100 km, respectively.

Figure Al displays the analytical admittance for the synthetic marg in with $w = 4$ km, $T = 100$ km. and $T_c = 32$ km. Density values arc 1030, 2800, and 3400 kg/m^3 for ρ_w, ρ_c, and ρ_m, respectively. Wc can see that the. absolute value of the admittance has peaks for $k = m\pi/T$, except for $k = O$; wc can also see that the amplitude never decays, reaching a constant value upon which the peaks are superimposed. Wc have. also plotted the "unwrapped" or pseudophase which is the phase with the π discontinuities removed. We have fitted two straight lines to this pseudophase, dividing the k range in two sectors: $k<0.05$ km^{-1} and $k>0.05$ km^{-1}. Wc see that the line.ar fit for high wavenumbers is 101 km, very c1osc to the real value of T which is 100 km. The phase spectrum appears to be a robust recorder of margin morphology and relative position of gr avity and bathymetry. For this reason we applied the reference phase to the observed admittance.

In Figure A2, wc have artificially shifted the gravity profile. in the previous example try 100 km to the left with respect 10 the bathymetric profile. This was done to simulate the possibility of incorrect bathymetry as we arc investigating in this paper. The plot of admittance phase shows regularly spaced discontinuities of π and 2π. While the log amplitude of admittance component is unaffected, the 2π discontinuities ar isc from the artificially imposed lack of compensation.

Figure A3 displays a profile along, latitude. 65°S. Note that the gravity and topography maxima and minima arc not coincident as would be the case for perfectly compensated and homogenous margin. The admittance amplitude of this profile does 1101 decay with increasing wavenumber as we observed in Figure Al. in fact, the admittance spectrum becomes highly en alit at large wavenumbers and the real component bc.come.s negative.

In Figure A4, we have modeled the gravity profile of Figure A3 using the. topography of Figure A3 and adjusting the size and location of low-density bodies to simulate sediment accumulation. The objective was to show the effect of imper feel compensation in the absence of measurement noise.

We see that the spectra of the modeled profile compare well with those of the observed profile with tbc occurrence of π and 2π phase. discontinuities in [hc phase component and negligible decay in the amplitude of the admittance function.

We conclude that the 2π discontinuities can be attributed to departures from the model of compensation. The average of several profile.s from a continental margin will display a deer case in amplitude with wavenumber, but this is due to the, averaging of irregularities in the real and imaginary spectral components and not to physical realities such as waler depth.

Acknowledgments. We wish to thank Bill Haxby for his contribution of the Geosat gravity field and the men of the NRL detachment at Pautuxent River Naval Air Station for the countless hours which they devoted to flying and maintaining the P-3 Orion 674. We also which [o thank Hank Fleming, John Brozena, Mary Peters, Skip Kovacs, of NRL and Carol Raymond, and Capt. Javier Valladares of the SHIN for their efforts in gathering the data sets. Not least we wish to thank Bill Hinze, Editor of JGR, for his infinite patience and Paul Wessel and Walter Smith for providing the GMT display sol-l Wale. This effort was supported by NSF grants DPP-85-17635 and 1)1'1'-87-1 9147, NASA Geodynamics and Geopotential Fields Programs suppoted by UPNS 465 and 579, the Instituto Antartico Argentino, the Servicio de Hidrografia Naval and Columbia University.

References

AnZone, International coordination of oceanographic research within the Antarctic zone, meeting report, I .an iont-Doherty Earth Obs., Palisades, N.Y., 1989.

Behrendt, J. C., Geophysics and geology of petroleum resources, in *Mineral Resources Potential of Antarctica, Antarcti. Res. Ser.*, vol. 51, edited by G. A. M. Dreschhoff, pp. 163-174, AGU, Washington, D.C., 1990.

Bell, R. E., J. Brozena, W. Haxby, and 1. L. LaBrecque, Continental margins of the western Weddell Sea: Insights from airborne gravity and Geosat derived gravity, in *Contributions to Antarctic Research 1, Antarct. Res. Ser., vol. 50,* edited by D.E. Hayes, pp. 91-102, AGU, Washington, D.C., 1990.

Brozena, J. M., A preliminary analysis of the NRL airborne gravimetry system, Geophysics, 49, 1060-1069, 1984.

Brozena, J. M., and M. F. Peters, An airborne gravity study of eastern North Carolina. *Geophysics, 53,245-253, 1988.*

Brozena, J, M., J. L. LaBrecque, R. Bell, and C. Raymond, An airborne gravity survey of the western Weddell Sea, *Eos Trans. AGU, 68, 1459,* 1987.

Cande, S.C., J. L. LaBrecque, R.L. Larson, W.C. Pitman 111, X. Golovchenko, and W.F. Haxby, *Magnetic Lineations of the* World's *Ocean Basins*, American Association of Petroleum (ecologists, Tulsa, Okl., 1989.

del Valle, R. A., and N. H. Forcade, La cuenca sedimentaria pos-Triasica dc extremo nororiental dc la Peninsula Antarctica, 323, 24 pp., Contrib. Cient. inst. Antart. Argentino, Buenos Aims, 1986.

del Valle, R. A., M.-l'. Diaz, J.C. Febrer, N. Fourcade, H.G. Fournier, J.C. Gasco, M.A. Keller, F. Medina, 11. Nunez, and M.C. Pomposiello, Mid-Cretaceous boundary detected below the Seymour island and its tracing offshore along the northeastern coast of the Antarctic

Peninsula by magnetotelluric measurements, *Acta Geod. Geophys. Montan. Hung.*, 2.7(2-4), 265-286, 1988.

Dorman, L. M., and B.T.R. Lewis, Experimental isostasy, 1, Theory of the determination of the Earth's isostatic response to a concentrated load, *J. Geophys. Res.*, 75,3357-3365, 1970.

Elliot, D.H., Tectonic setting and evolution of the James Ross Basin, northern Antarctic Peninsula, *Mem. Geol. Soc. Am., 169, 541-555,* 1988.

Farquharson, G. W., Late Mesozoic sedimentation in the northern Antarctic Peninsula and its relationship to the southern Andes, *J. Geol. Sot. London,* 139, 721-727, 1982.

Farquharson, G.W., Evolution of Late Mesozoic sedimentary basins in the northern Antarctic Peninsula. in *Antarctic Earth Science,* edited by R.L. Oliver, P.R. James, and J. B. Jago, pp. 323-327, Cambridge University Press, New York, 1983.

González-Ferrán, 0., The Larsen Rift: An active extension fracture in West Antarctica, in *Antarctic Earth Science,* edited by R. 1. Oliver, P.R. James, and J. J\. Jago, pp. 344-351, Australian Academy of Science, Canberra, 1983.

Gordon, A. L., and the Ice Station Weddell Group, Weddell Sea Exploration from Ice Station, *Eos Trans. AGU,* 74, 11, 121, 1993a.

Gordon, A. L., B.A. Huber, H.H. Hellmer, and A. Ffield, Deep and bottom water of the Weddell Sea's western rim, *Science,* 262, 95-97, 1993b.

Grikurov, G., V. Traube, G. Leitchenkov, N. Aleshkova., A. Golynskji, Structure and evolution of sedimentary basins in the Weddell province, paper presented at 1st Conferencia Sobre Geofisica, Geodesia e Investigacion Espacial Antarcticas, CONICET, Buenos Aim, 1990,

Grunow, A. M., D.V. Kent, , and I. W. I). Dalziel, Mesozoic evolution of West Antarctica and the Weddell Sea Basin: New paleomagnetic constraints, *Earth Planet. Sci. Lett., 86,* 16-26, 1987.

I Iartman, R.R., D.J. Teskey, and J.L. Freidberg, A system for rapid digital aeromagnetic interpretation, *Geophysics,* 36, 891-918, 1971.

1 Iaxby, W., Organization of oblique seafloor spreading into discrete, uniformly spaced ridge segments: Evidence from the Geosat altimeter data in the Weddell Sea, *Eos Trans. AGU,* 69(44), 1155, 1988.

Haxby, W., and D. E. 1 layes, Free-air gravity of the Southern Ocean derived from Seasat and Geosat altimeter data: Circum-Antarctic to 30°S, in *Marine Geological and Geophysical Atlas of the Circum-Antarctic to 30°S, An/arc/. Res. Ser.,* vol. *54,* edited by D.E. Hayes, pp. 11-19. AGU, Washington, D.C., 1991.

Johnson, G.L., J.R. Vanney, D.J. Drewry, and G. Robin, General bathymetric chart of the oceans (GEBCO), Can. Hydrogr. Serv., Ottawa, 1983.

Kadmina, I.N., R.G. Kurinin, V.N. Masolov, and G. Ii. Grikurov, Antarctic crustal structure from geophysical evidence: A review, in *Antarctic Earth Science,* edited by R.L. Oliver, R.R. Jones, and J.B. Jago, pp. 498-502, Cambridge University Press, New York, 1983.

Kavoun, M. and 0. Vinnikovskaya, Seismic stratigraphy and tectonics of the northwestern Weddell Scs (Antarctica) inferred from marine geophysical surveys, Tectonophysics, 240,299-341, 1994.

Karner, G.D., and A. B. Watts, On isostasy at Atlantic-type continental margins, *J. Geophys. Res.*, 87, 2923-2948, 1982.

Keller, M. A., arid M."I'. Diaz, Estudio geofisico en la cuenca dc Larsen, Antartida, paper presented at 1st Congress, Brazilian Geophys. Sot., Rio dc Janeiro, 1989.

Keller, M.A., J.H. Nunez, and M.'l'. Diaz, Some morphological aspects of the northwest section of the Weddell Sea Basin, *Contrib. 313, 9 pp.,* Inst. Antarct. Argentino, Buenos Aim., 1985.

I aBrecque, J.] .., and P.F. Barker, Age of the Weddell Basin, *Nature,* 290,489-492, 1981.

LaBrecque, J.L., et al., South Atlantic Oman and adjacent Antarctic margin, in Ocean Margin Drilling Program, Regional Atlas Series, *Atlas 13, 21* sheets, Marine Science International, Woods Hole, Mass., 1986.

LaBrecque, J.L., et al., USAC aerosurvey results for the Weddell Basin, part I, paper presented at 28th Intonational Geological Congress, IUGG, Washington, D.C., 1989.

Lewis, B.T.R., and L.M. Dorman, Experimental isostasy, 2, An isostatic model for the United States derived from gravity and topographic data, *J. Geophys. Res.*, 75,3367-3386, 1970.

Ludwig, W.J., et al., Tertiary and Cretaceous paleoenvironments in the southwest Atlantic Ocean, preliminary results of Deep Sea Drilling Project Leg 71, *Geol. Soc. Am. Bull., 91,655-664, 1980.*

Macdonald, D.I.M., P.F. Barker, S.W. Garrett, J.R. Garrett, J.R. Ineson, D.Pirrie, B.C. Storey, A.G. Whitham, R.R.F. Kinghorn, and J.E.A. Marshall, A preliminary assessment of the hydrocarbon potential of the Larsen Basin, Antarctica, Mar. *Petrol. Geol.*, 5,34.54, 1988.

Marks, K. M., and D.C. McAdoo, Gravity field over the Southern Ocean from Geosat, *Rep. MGG-6*, Natl. Geophys. Data Cent., Boulder, Colo., 1992.

Maslanyj, M.P.. and B.C. Storey, Regional aeromagnetic anomalies in Ellsworth Land: Crustal structure and Mesozoic microplate boundaries with West Antarctica, *Tectonics*, 9, 1515-1532, 1990.

Maslov, V.N., Stroenie magnitoaktivnogo fundamenta jugo-vostochnoy chasti bassein a moria Weddella / Structure of the magnetic basement in the southeastern part of Weddell Sea Basin, in *Geofiziicheskie issledovania* v *An/ark/tie* (Geophysical *Survey* in Antarctica), pp. 14-28, Research Institute of Arctic Geology, Leningrad, 1960.

McKenzie, D., and C. Bowin, The relationship between bathymetry and gravity in the Atlantic Ocean, *J. Geophys. Res.*, 81, 1903-1915, 1976.

Nabighian, M. N., The analytic signal of two-dimensional magnetic bodies with polygonal cross-section: Its properties and use for automated anomaly interpretation, *Geophysics, 37, 507-517, 1972,*

Natland, M.L. . . E.P. Gonzalez, A. Canon, and M. Ernst, A system of stages for the cone.laticm of Magallanes Basin sediments, *Mem. Geol. Soc Am.*, 139, 126 pp., 1914.

Olivero, E., R.A. Scasso, and C.A. Rinaldi, Revision del grupo Marambio, Isla James Ross, Antartida, 331,27 pp., Contrib. Cient. del inst. to Antartct. Argentino, Buenos Aires, 1986.

Parra, J. C., and G. Yanez, Reconocimiento Aeromagntico en la Peninsula Antartica y mares circundantes i Integracion de informacion obtenida a diferentes alturas, *Publicacion especial sobre temas antarcticos*, Congr. Geol. Chileno, Santiago, 1988.

Parra, J. C., C). Ganzalez-Ferran, and J. Bannister, Aeromagnetic survey over the South Shetland Islands, Bransfield Strait and part of the Antarctic Peninsula, *Rev. Geol. Chile, 23,3-20,* 1984.

Phillips, J, I), Statistical analysis of magnetic profiles and geomagnetic reversal sequences, Ph.D thesis, 134 pp., Stanford Univ., Stanford, Calif, 1975.

Renner, G. G.B., L.J.S. Sturgeon, and S.W. Garrett, Reconnaissance gravity and aeromagnetic surveys of the Antarctic Peninsula, *Sci. Rep. 110,* British Antarctic Survey Cambridge, 1985.

Rinaldi, C. A., The Upper Cretaceous in the James Ross island Group, in *Antarctic Geosciences*, edited by C. Craddock, p. 281 -286, University of Wisconsin Press, Madison, 1982.

Shure, L., and R.L. Parker, An alternative explanation for intermediate wavelength magnetic anomalies, *J. Geophys. Res.*, 86, 11 ,6(KI 11,608, 1981.

Schouten, H., and K. McCamy, Filtering marine magnetic anomalies, *J. Geophys. Res.*, 77, 7089-7099, 1972.

Spector, A., and F.S. Grant, Statistical models for interpreting aeromagnetic data, *Geophysics, 35, 263-302, 1970.*

Steckler, M.S., and A.B. Watts, Subsidence of the Atlantic-type continental margin off New York, *Earth Planet. Sci. Lett.*, 41, 1-13, 1978.

St. John, W., Antarctica-geology and hydrocarbon potential, in Future Petroleum Provinces of the World, edited by M. Halbouty, *AAPG Mere., 40,55-100,* 1986.

Treitel, S., W.G. Clement, and R.K. Kaul, The spectral determination of depths to buried magnetic basement rocks, *Geophys. J. Roy Astron. Sot.*, 24, 415-428, 1971.

Walcott, R. I., Flexual rigidity, thickness and viscosity of the lithosphere, *J. Geophys. Res.*, 7S, 3941-3954, 1970.

Walcott, R.I., Gravity flexure and rhc growth of sedimentary basins at a continental edge, Gee/. Sot. *of Am. [lull., 83, 1845-1848, 1972.*

Watts, A.B., An analysis of isostasy in the world's oceans, 1, Hawaiian - Emperor Seamount Chain, *J. Geophys. Res., 83,* 5989-6004, *1978.*

Watts, A.B., and S.F. Daly, Long wavelength gravity and topographic anomalies, *Annu.* Rev. *Earth Planet. Sci., 9, 415-448, 1981.*

Wessel, *P.,* and W. 11. F. Smith, Free software helps map and display data, *Eos Trans. AGU, 72,* 441, 445-446, 1991.

Whitham, A. G., and B.C. Storey, Late Jurassic-Early Cretaceous strike-slip deformation in the Nordenskjold Formation of Graham Land, *Antarct. Sci., 1,* 269-278, 1989.

J. I.. LaBrecque, Code YSG, NASA, Washington, DC 20037. (e-mail: jlabrecq@mtpe.hq.nasa.gov)

M.E. Ghidella, Instituto Antartico Argentino, Cerrito 12.48 1010 Buenos Aires, Argentino, (c-mail: marta@antar.org.ar)

(Received March 12, 1996; accepted March 19,1996.)

[1]Also at the Lamont-Doherty Earth Observatory of Columbia University

Paper number JB960175.
0148-0227/96/96JB-00175$05.00

USAC FLIGHTS

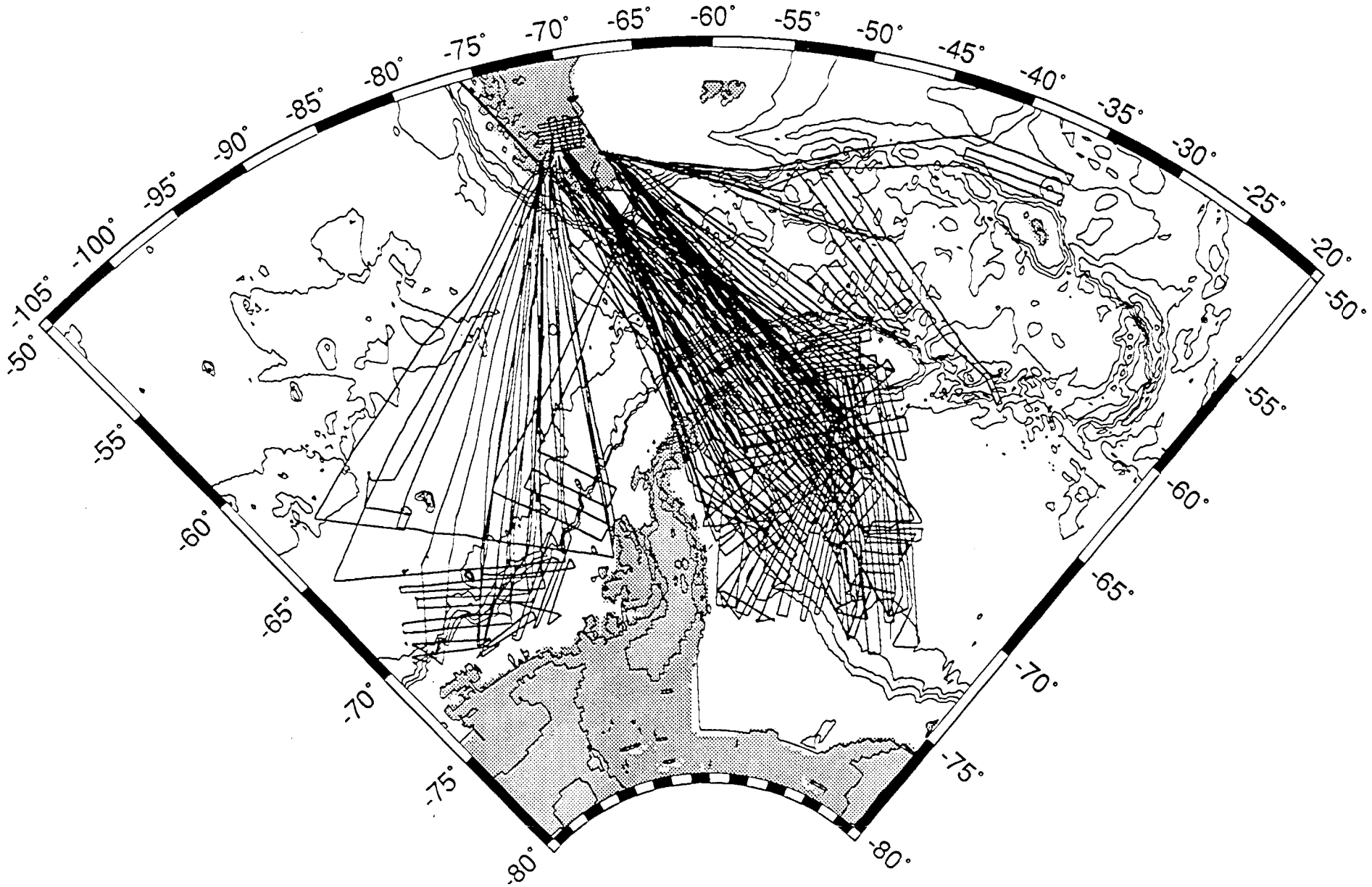

Figure 1. All USAC flights (1985-1989 field seasons). Bathymetric contours are plotted at 1000-m intervals. Antarctic Peninsula and South America are shaded.

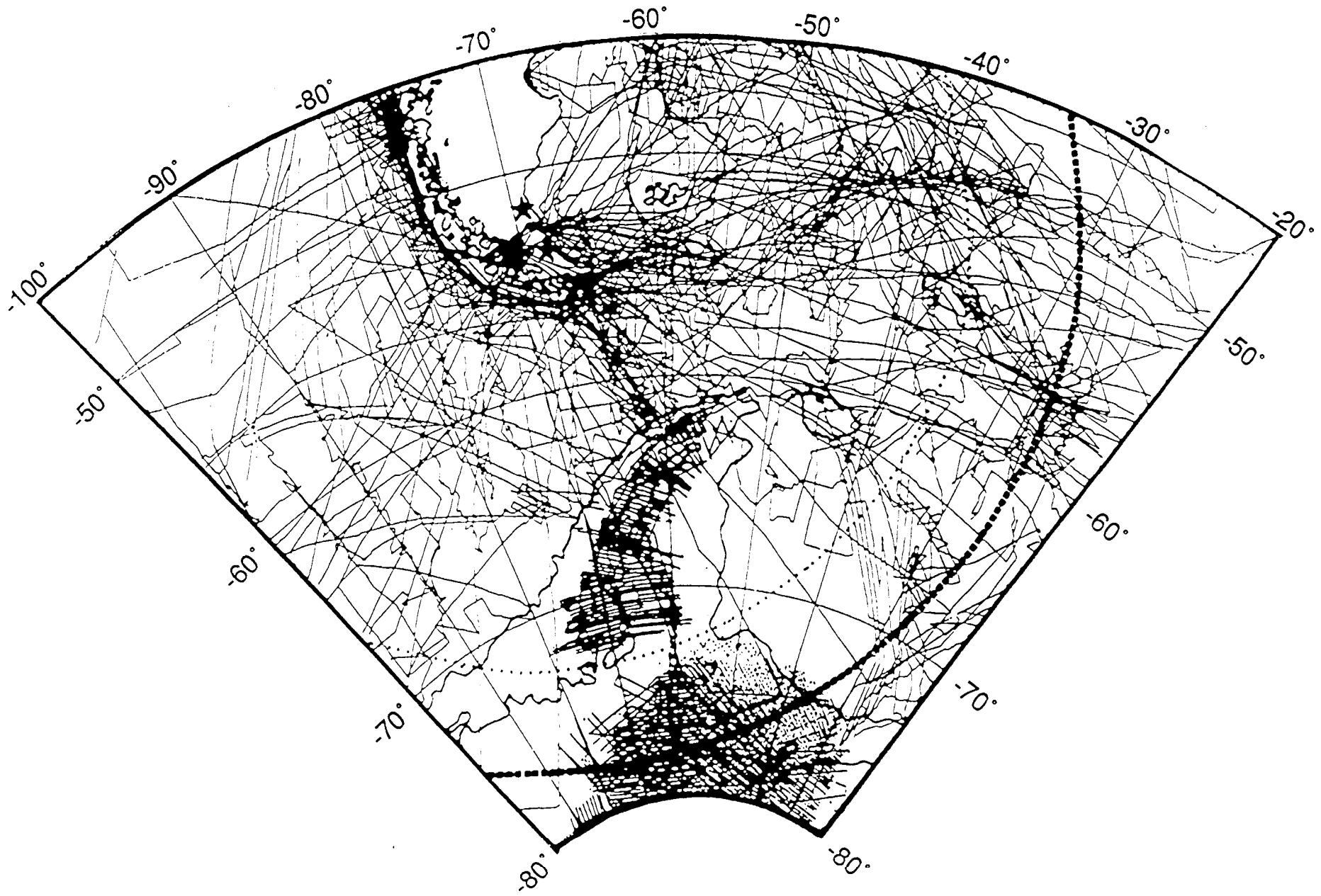

Figure 2. All geophysical data in the region prior to USAC. Compilation includes bathymetry, gravity, and magnetic measurements. Also shown as stipled lines are the 2400-and 3 000-nm range limits for aircraft departing from Tierra del Fuego (star). Stipled lines in southern Weddell Sea (below 70°S) arc Russian

Figure 2

FREE AIR GRAVITY

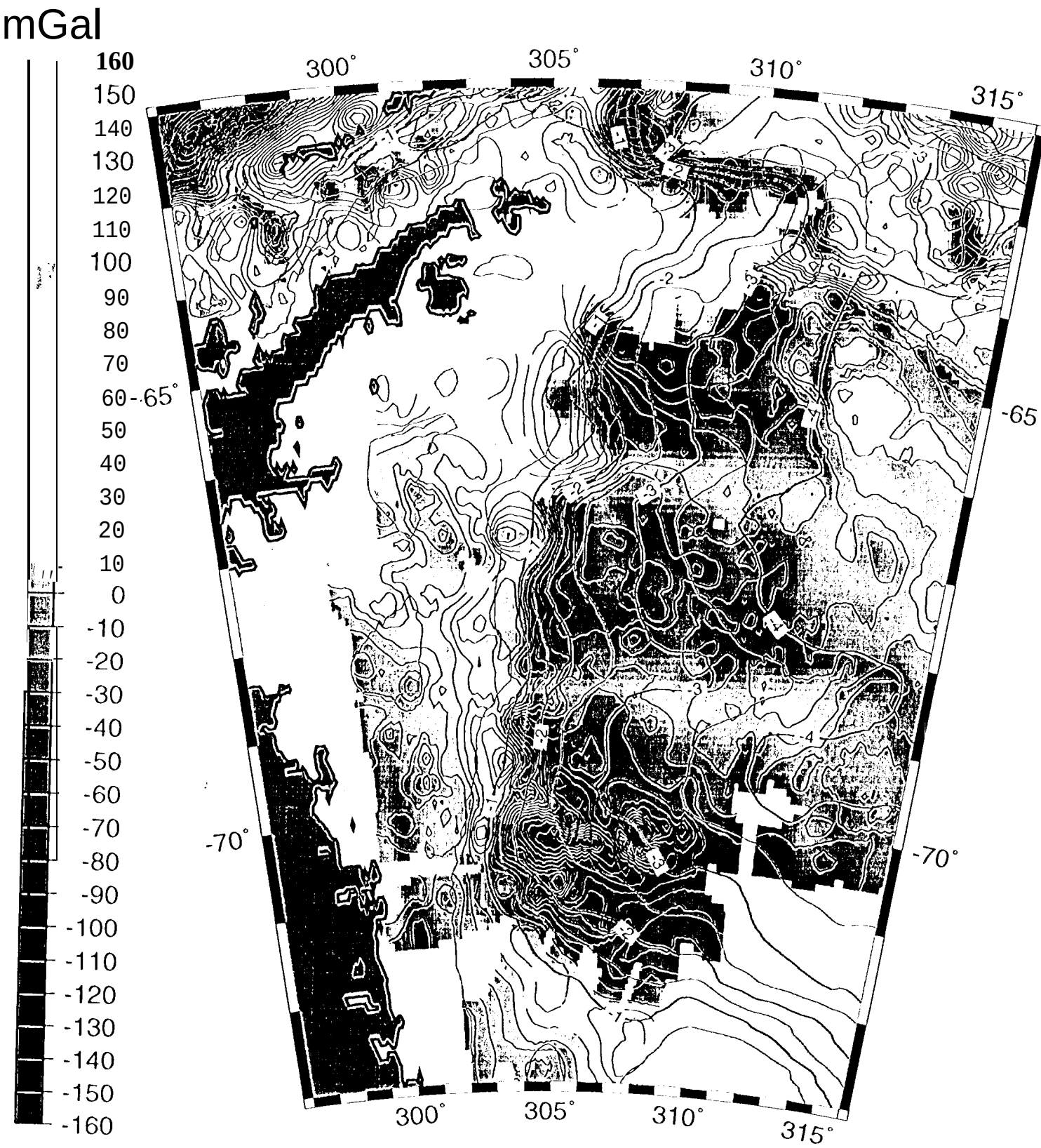

Plate 1a. Gravity field for the Weddell Basin using USAC aerogravity data base and the Geosat derived gravity field [*Haxby*, 1988, *Bell et* 01.,1990]. Revised bathymetry from Plate 2 is plotted in orange. Areas of no data are masked in gray. Coastline is delineated in red.

MAGNETIC ANOMALIES

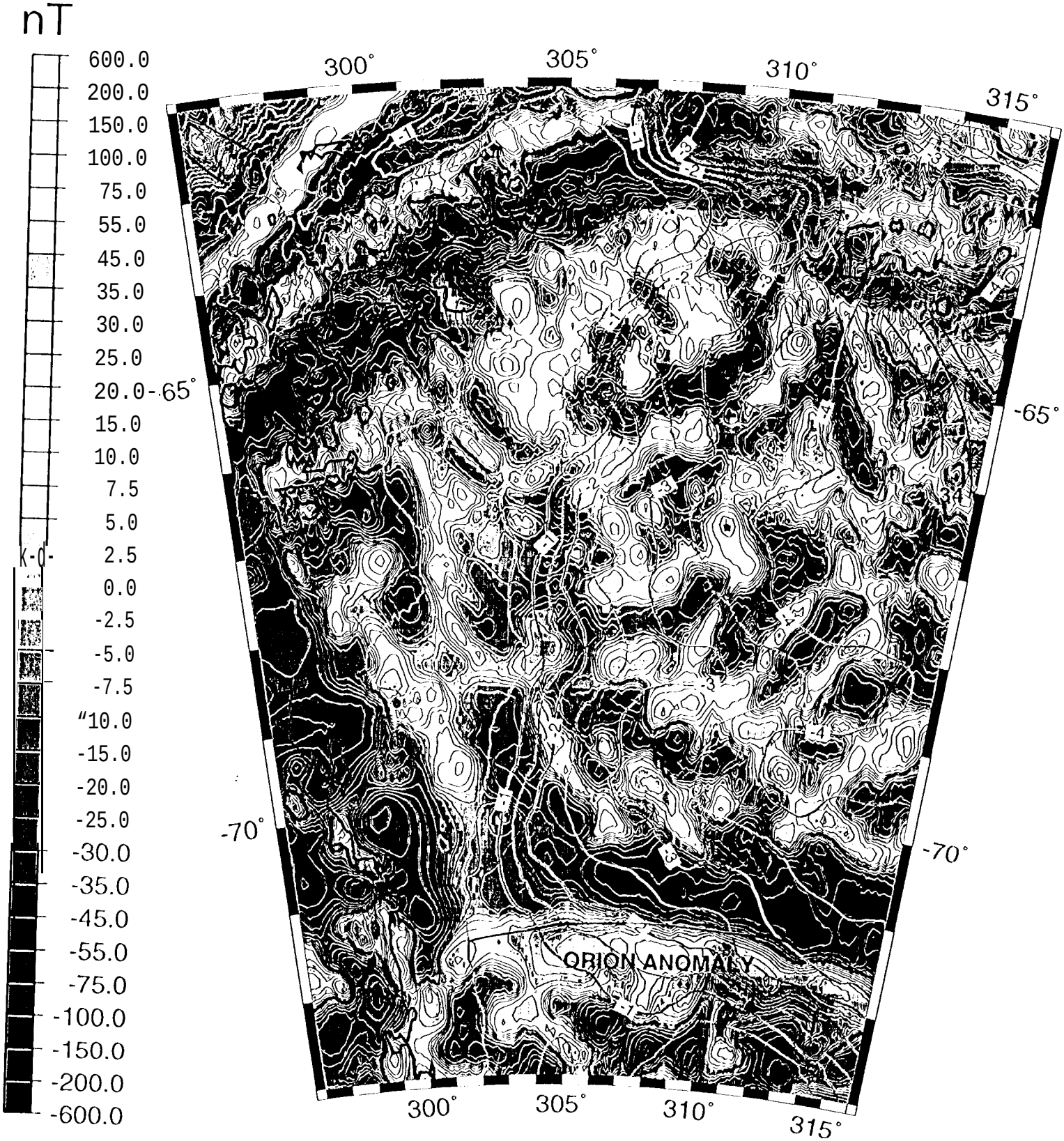

Plate 1b. Magnetic anomaly field of the Weddell Basin. Database includes all USAC flights, aerosurveys of *Renner et al, [198S], Mus1ov [1* 980] and marine data of *LaBrecque et al. [1986]. Revised* bathymetry from Plate 2 is },1oi[C.CI in orange. Also shown in darker red arc the tectonic lineations from *Cande et al. []* 989] *showing* the Orion Anomaly of the southern Weddell Basin and the *seafloor* spreading magnetic anomalies and fracture zone trends of the northern Weddell Basin with location of anomaly 34. Coastline is delineated in *rd*.

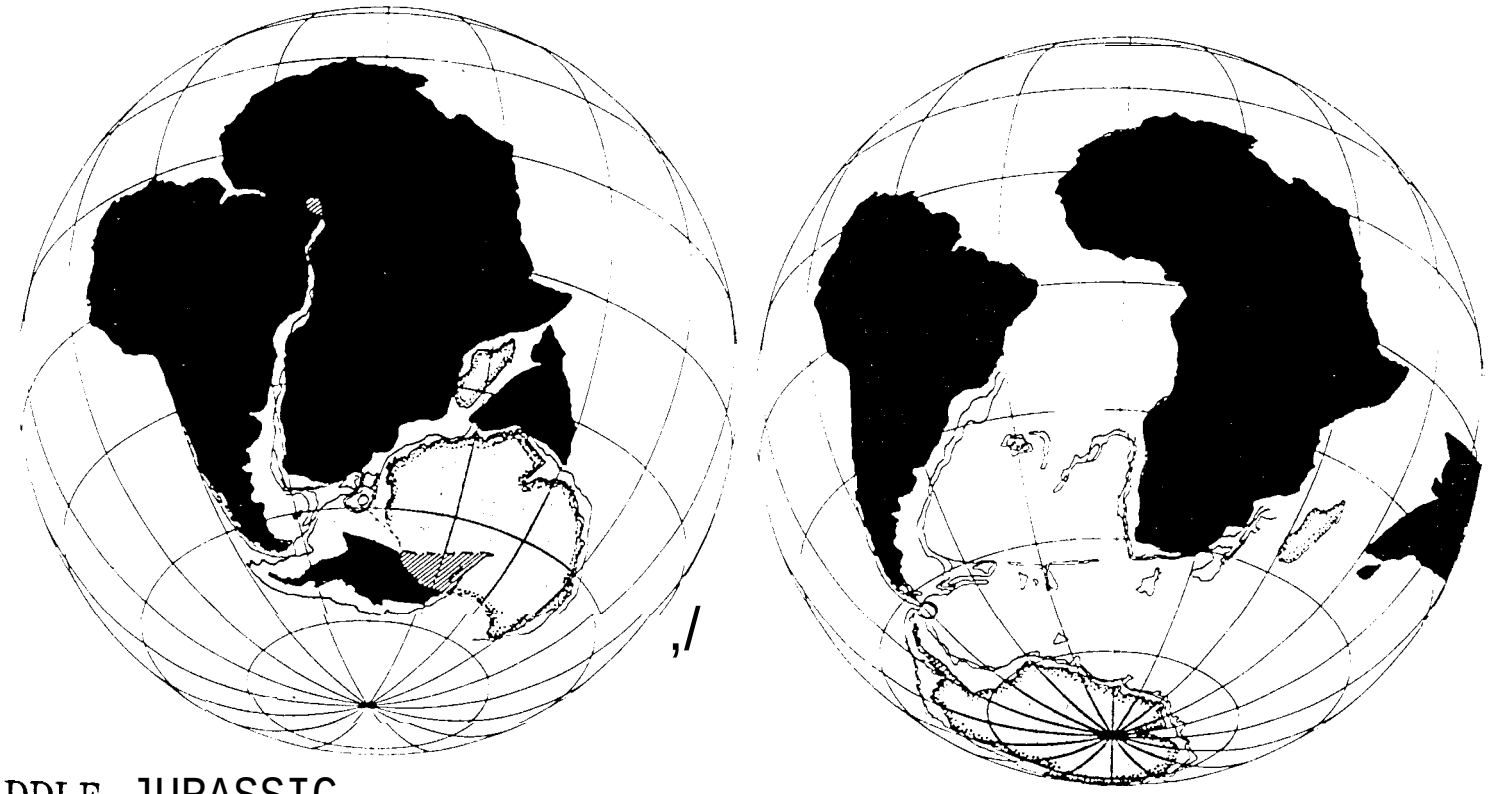

Figure 3. Reconstructions of the Weddell Basin for Jurassic and Jurassic Cretaceous Boundary based on seafloor spreading lineations *in the* Weddell Basin [from *Laßrecque et al., 19S 6].* Middle Jurassic reconstruction Shows the 'Ross Sea Basin (stipled area) overlapping the East Antarctic craton. Thousand meter contour intervals of margins and relevant oceanic rises are shown where appropriate.

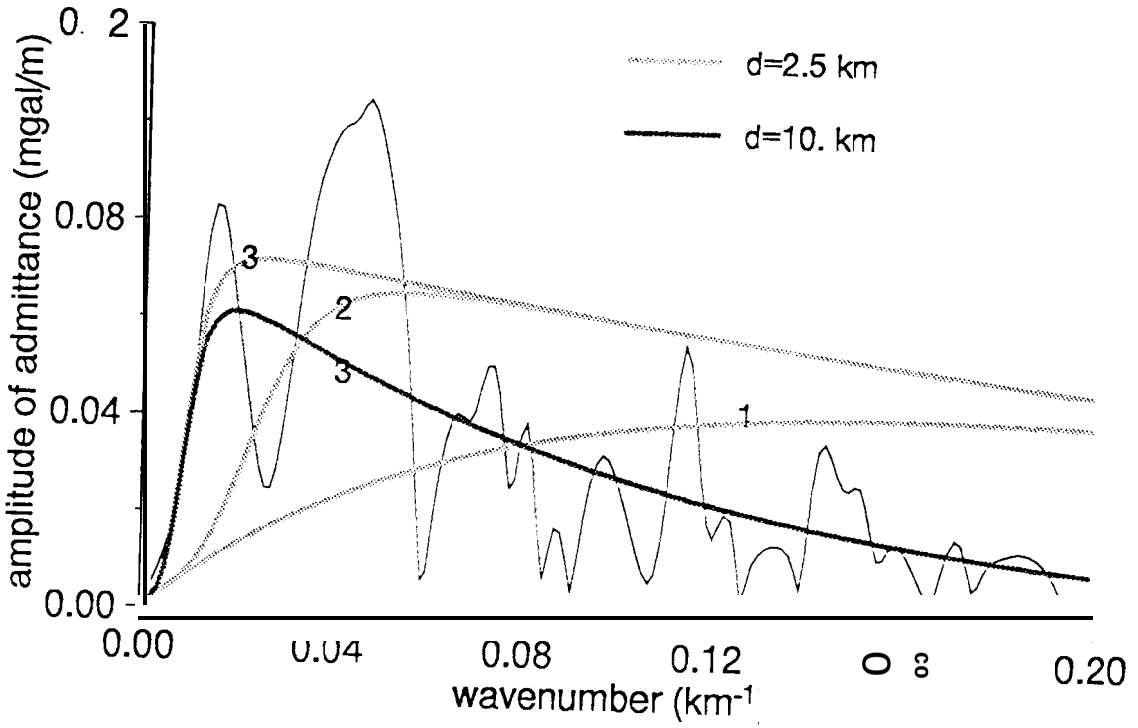

Figure 4. Log amplitude of the admittance function for northern reference area of the Weddell margin. Theoretical admittance functions for mean depths 2.5 and 10 km as indicated. Lithospheric elastic thicknesses are (1) 0 km, (2) 10 km, and (3) 40 km.

(a).

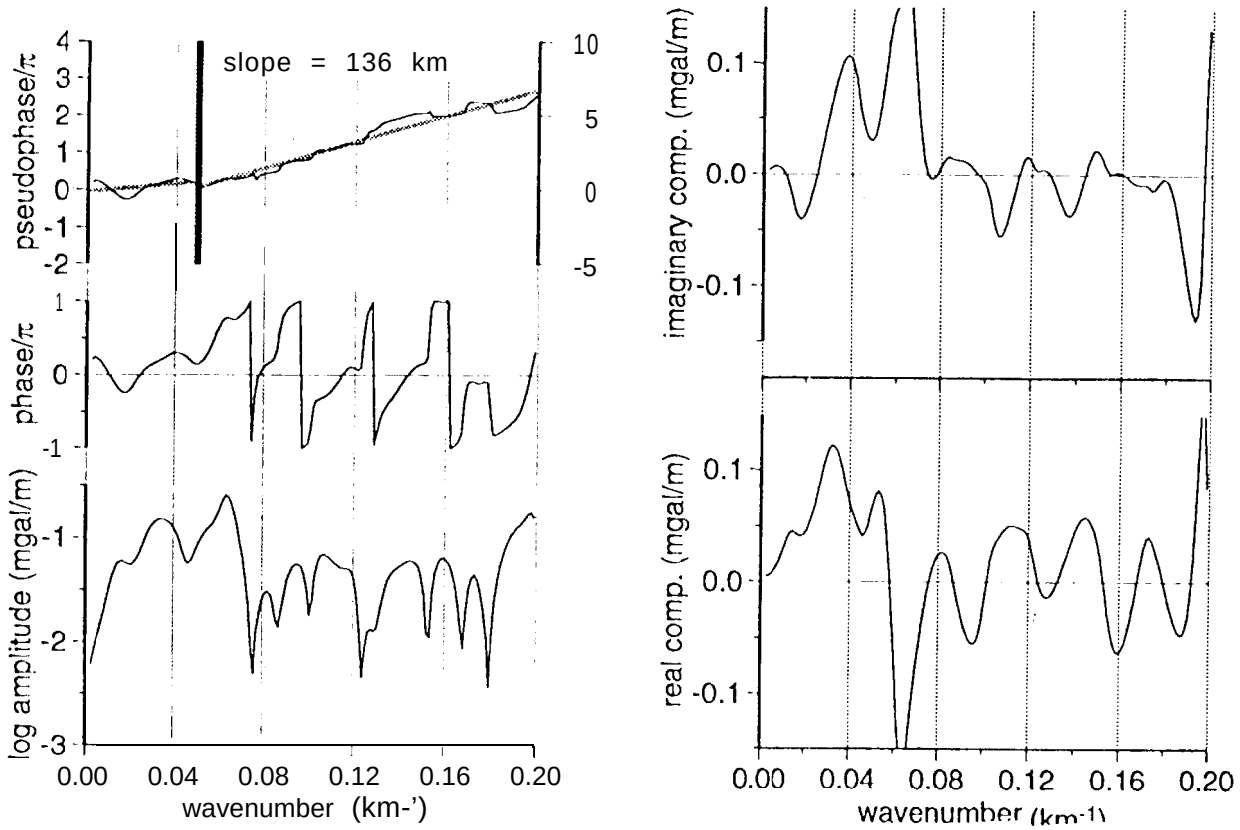

Figure 5a. Admittance function for observed profile at 65 .5°S. Note the occurrence of both π and 2π discontinuities in the phase. Note also that for high wavenumbers the phase slope is 136 km, approximately the width of the shelf slope in this profile.

(b).

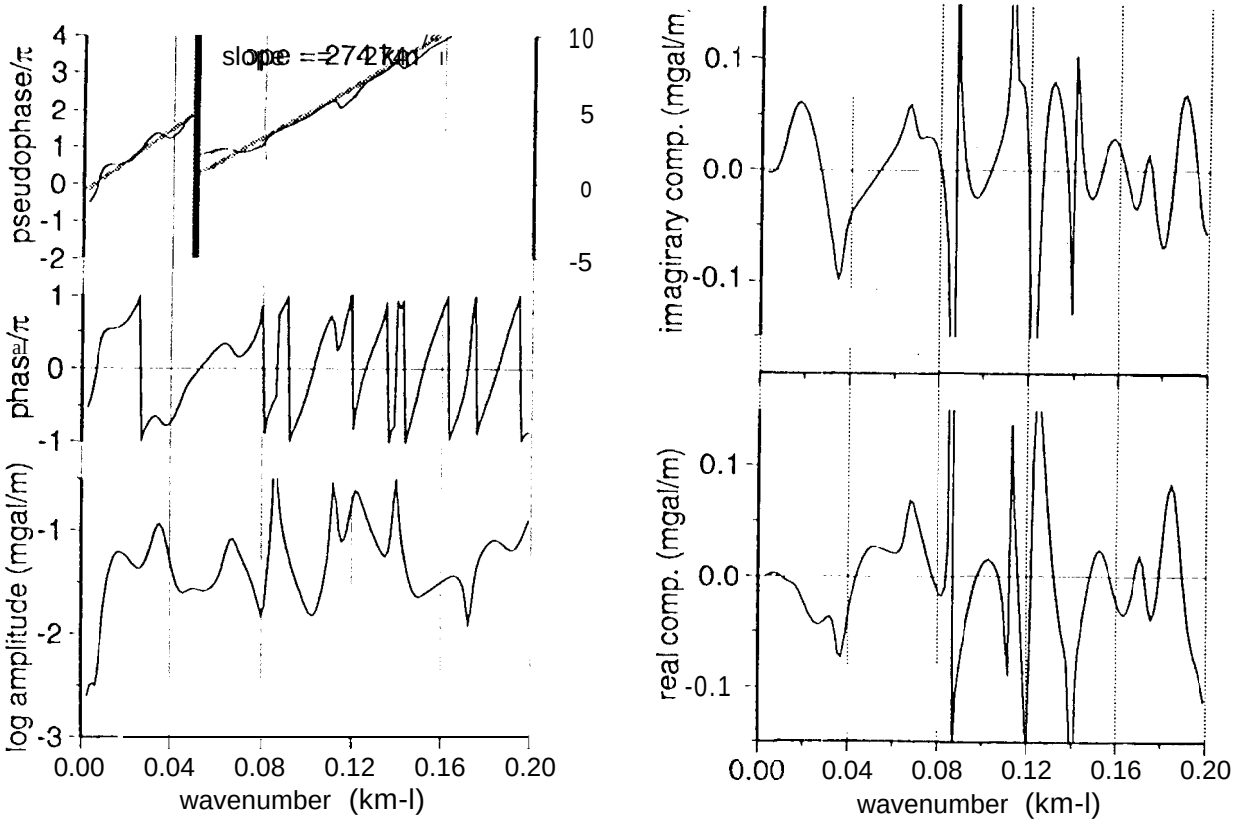

Figure 5b. Admittance function for observed profile at 68.4°S. Note the steeper phase shift at both low and high wavenumbers in the unwrapped phase for the southern margin versus the northern profile of Figure 5a.

REVISED BATHYMETRY

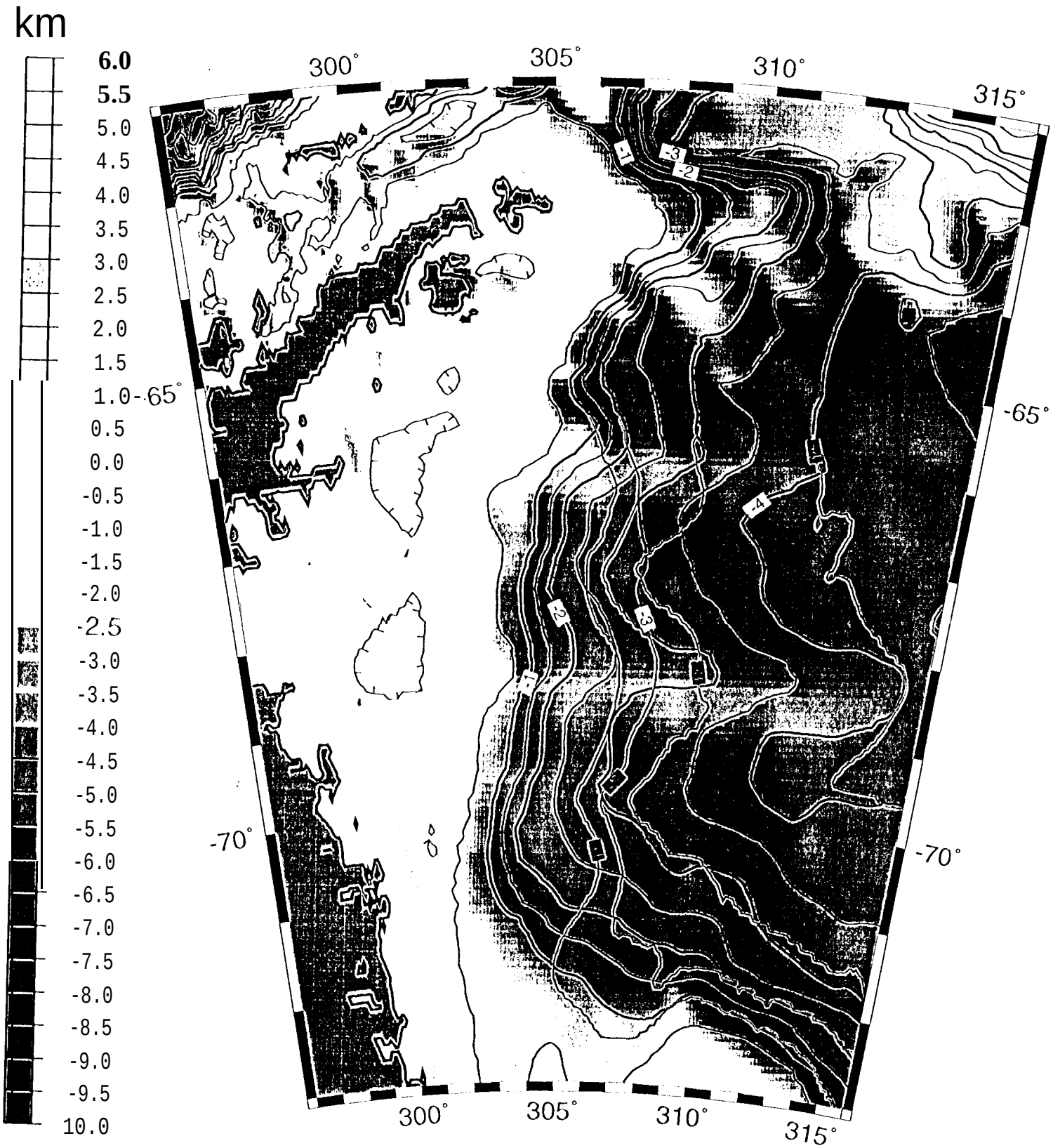

Plate 2. Revised bathymetry for the Weddell Basin derived from the admittance inversion. Older GEBCO contours arc displayed in red at a 1 -km contour interval over the region of revise.d bathymetry in the southwestern basin.

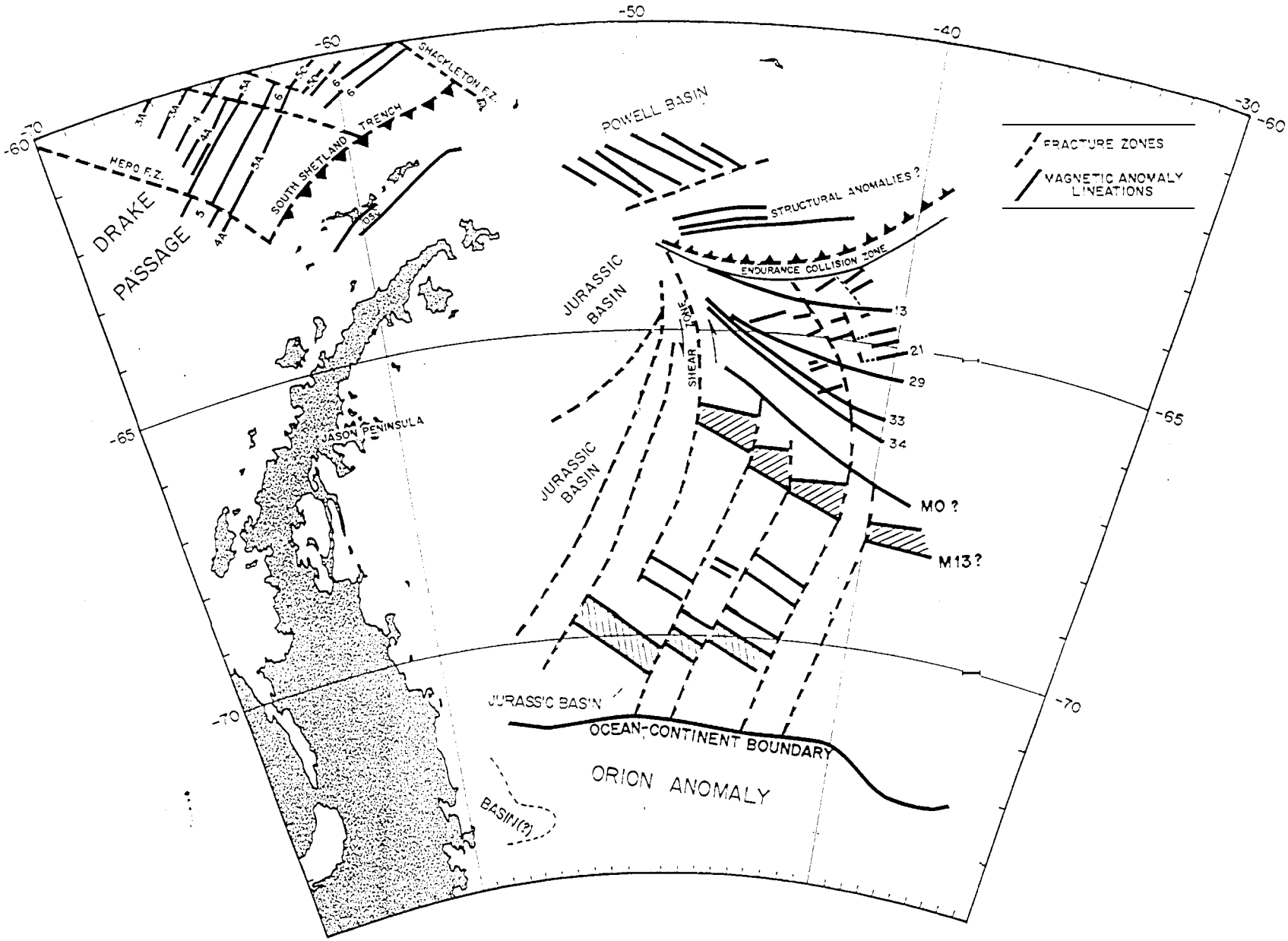

Figure 6. Tectonic map of the major isochrons, fracture zones, and magnetic lineaments.

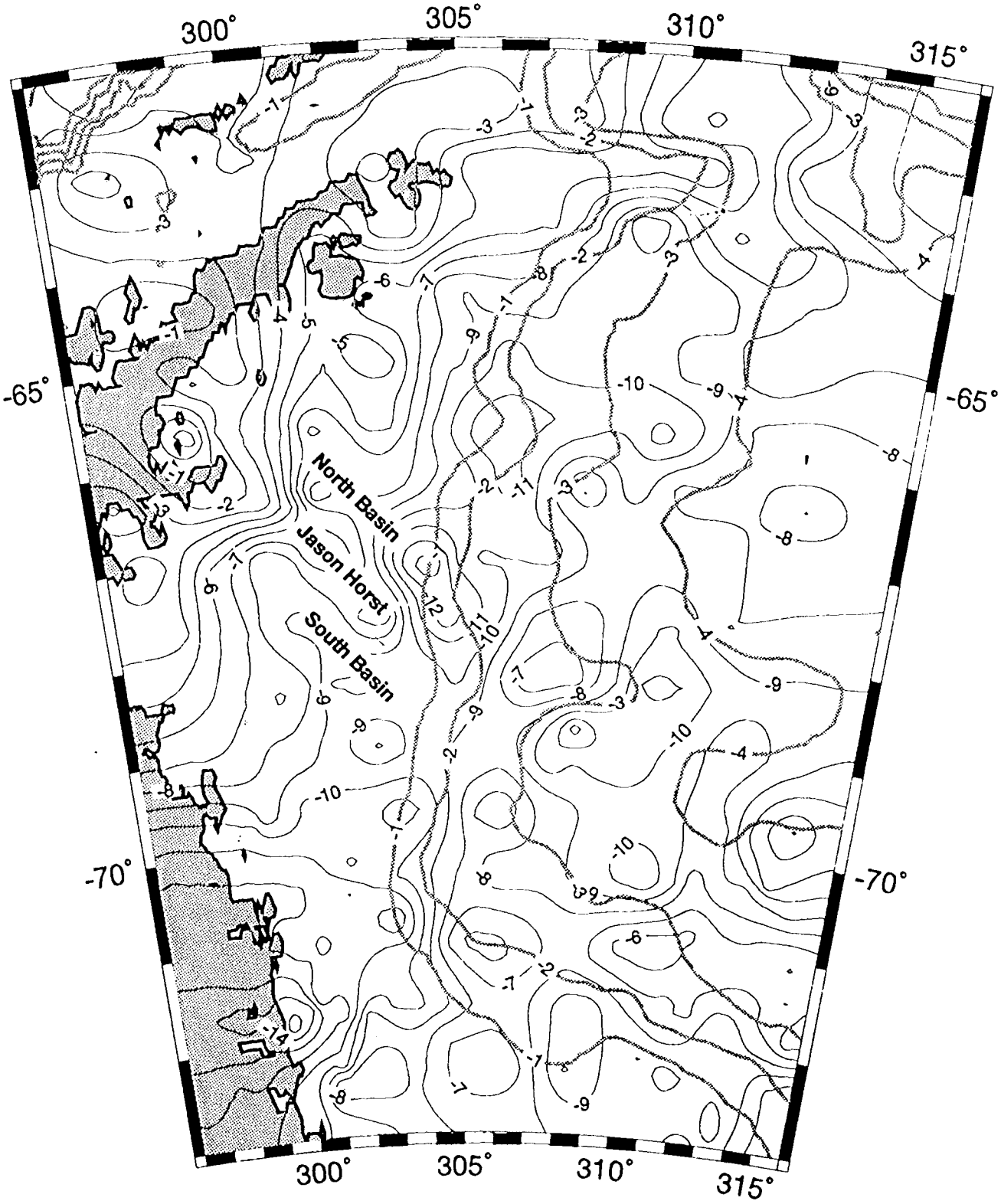

Figure 7. Depth to magnetic basement in the Weddell Basin. Contour interval is 1 km. Revised bathymetry is shown as thick grey lines at 1-km contour intervals. Magnetic base.mcnt estimates arc spurious over southern An[arctic Peninsula for lack of data.

ISOPACH OF NOB

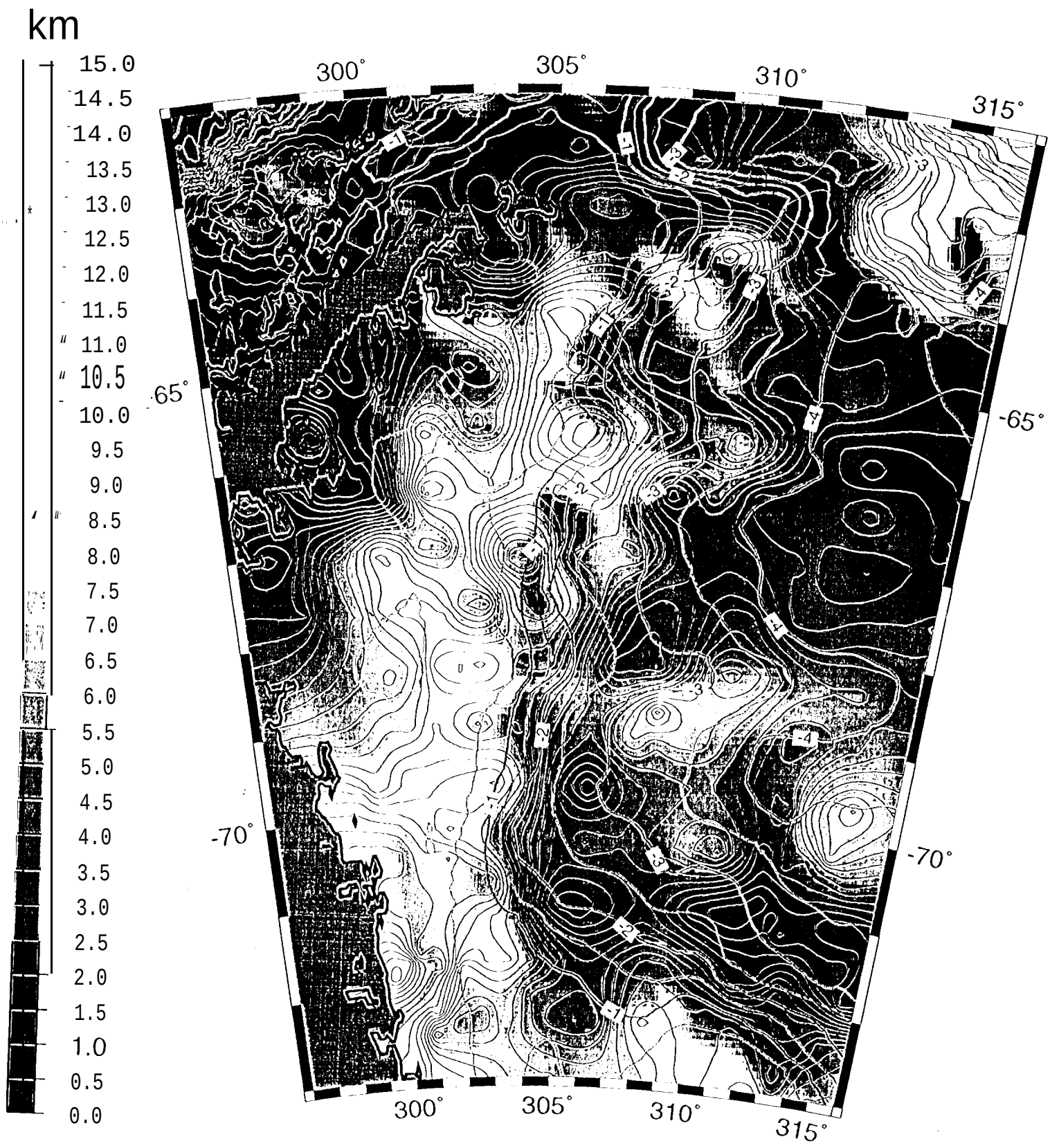

Plate 3. Estimated thickness of nonmagnetic overburden (sediment thickness) using revised bathymetry (Plate 2) and depth to magnetic basement (Figure 7). Revised bathymetry is plotted in orange at 1-km intervals. Land is masked in grey.

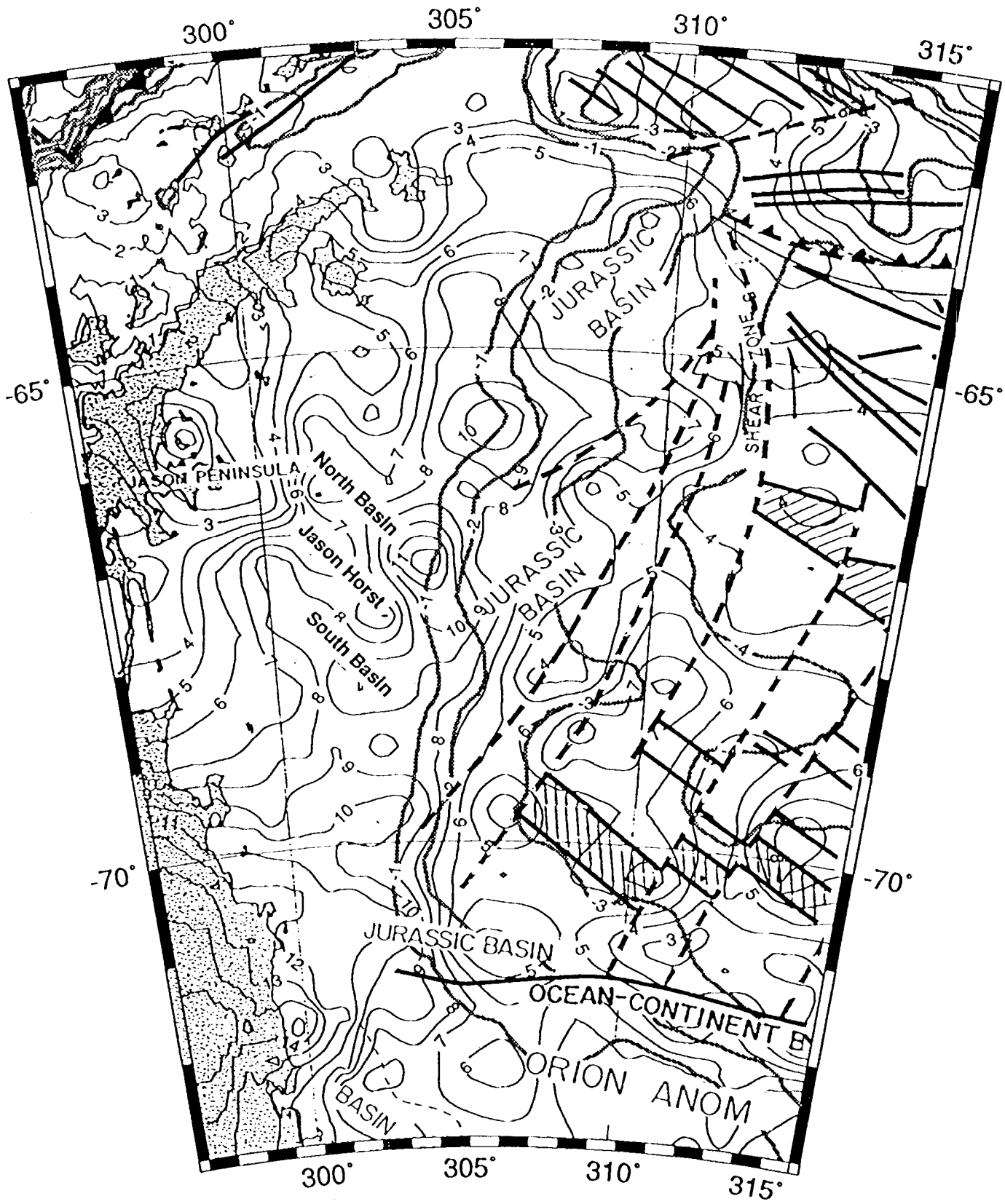

Figure 8. Same as Plate 3 with tectonic map of Figure 6 superimposed.

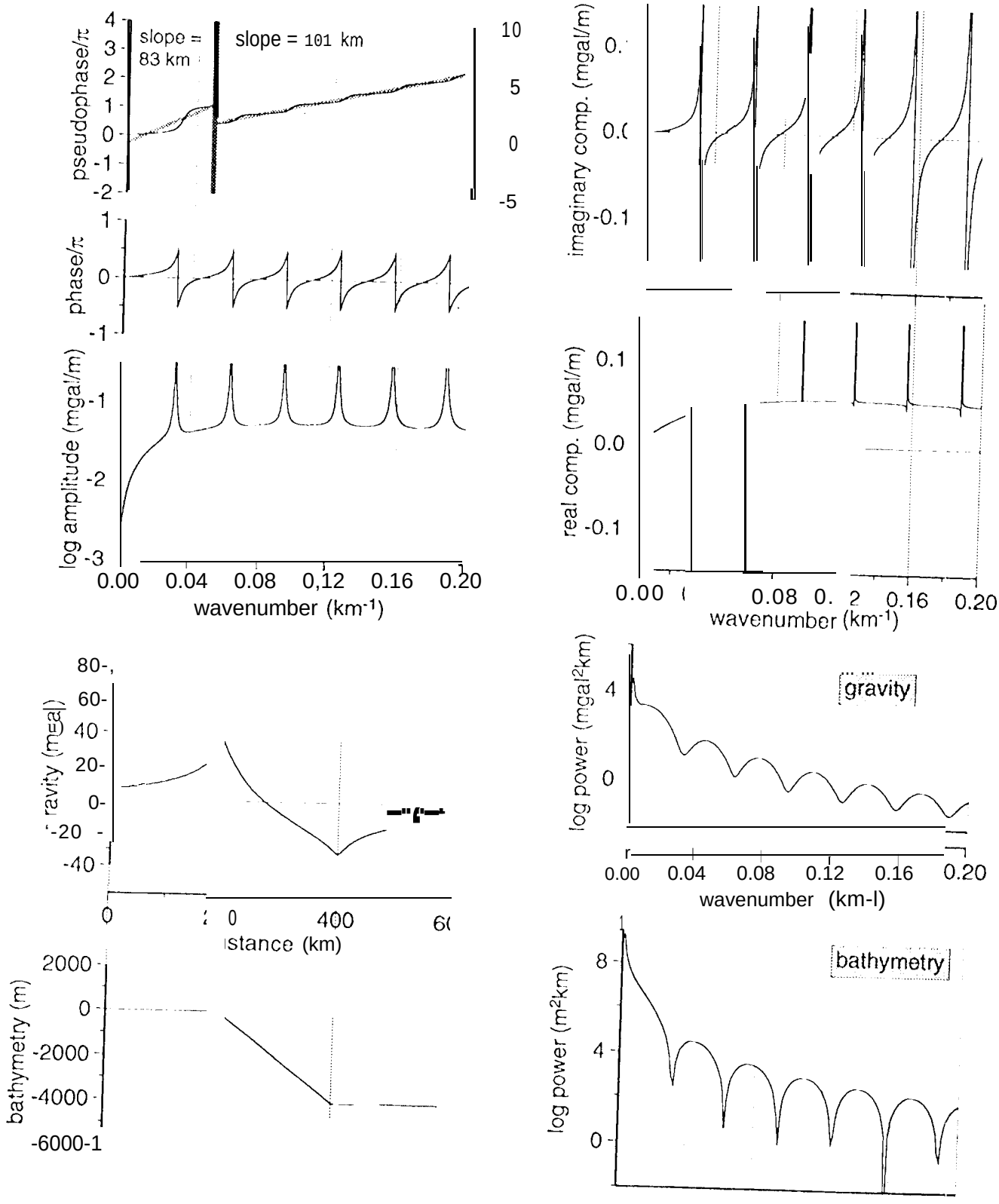

Figure A1. The analytically determined admittance for a model continental margin. Shelf slope half width is 100 km, and water depth is 4 km with local isostatic compensation.

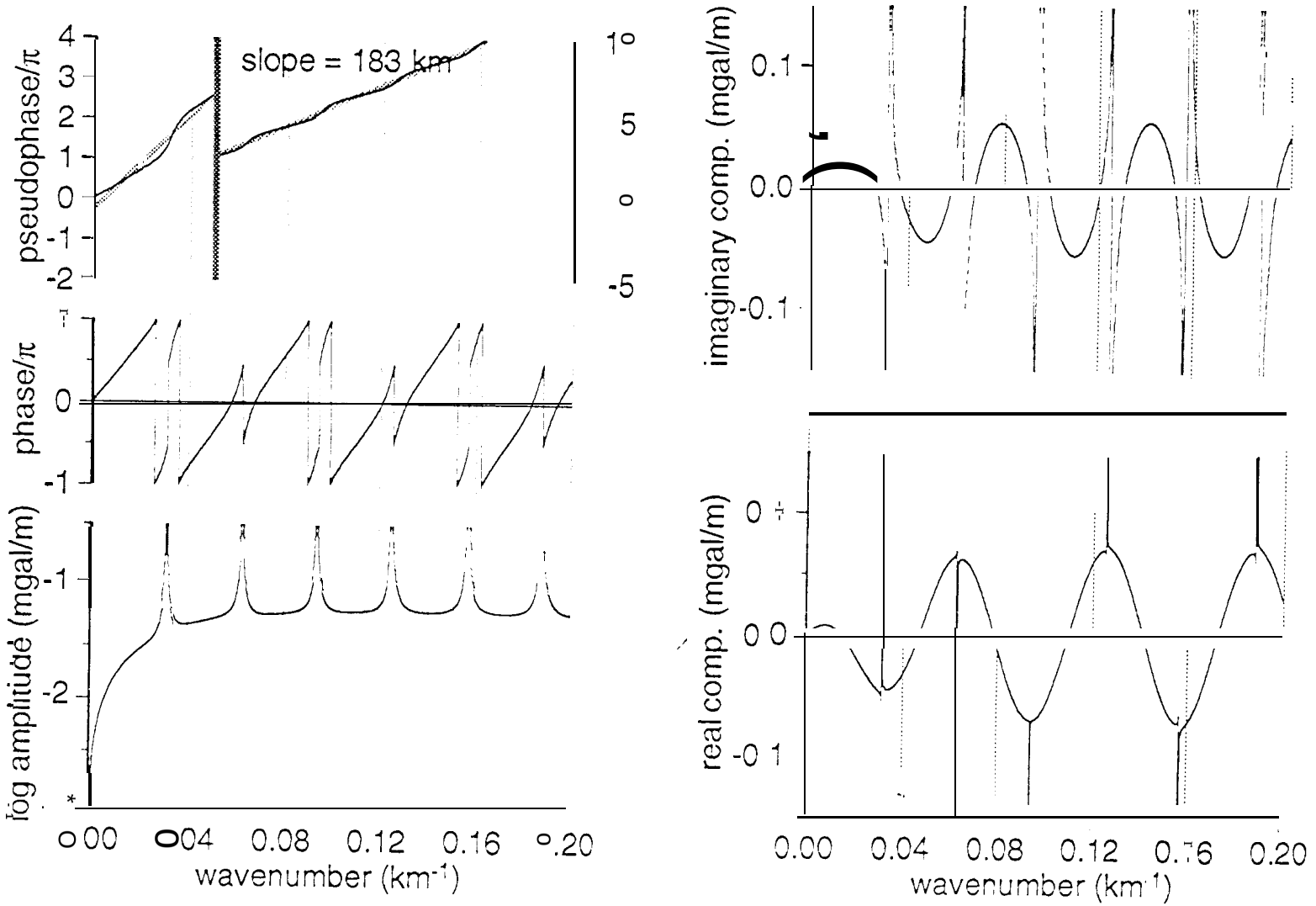

Figure A2. Admittance of the model in Figure A1 in which the gravity has been shifted 100 km to the left with respect to the topography profile. Note the appearance of 2π discontinuities in the phase and the steepening of the unwrapped phase as predicted by theory.

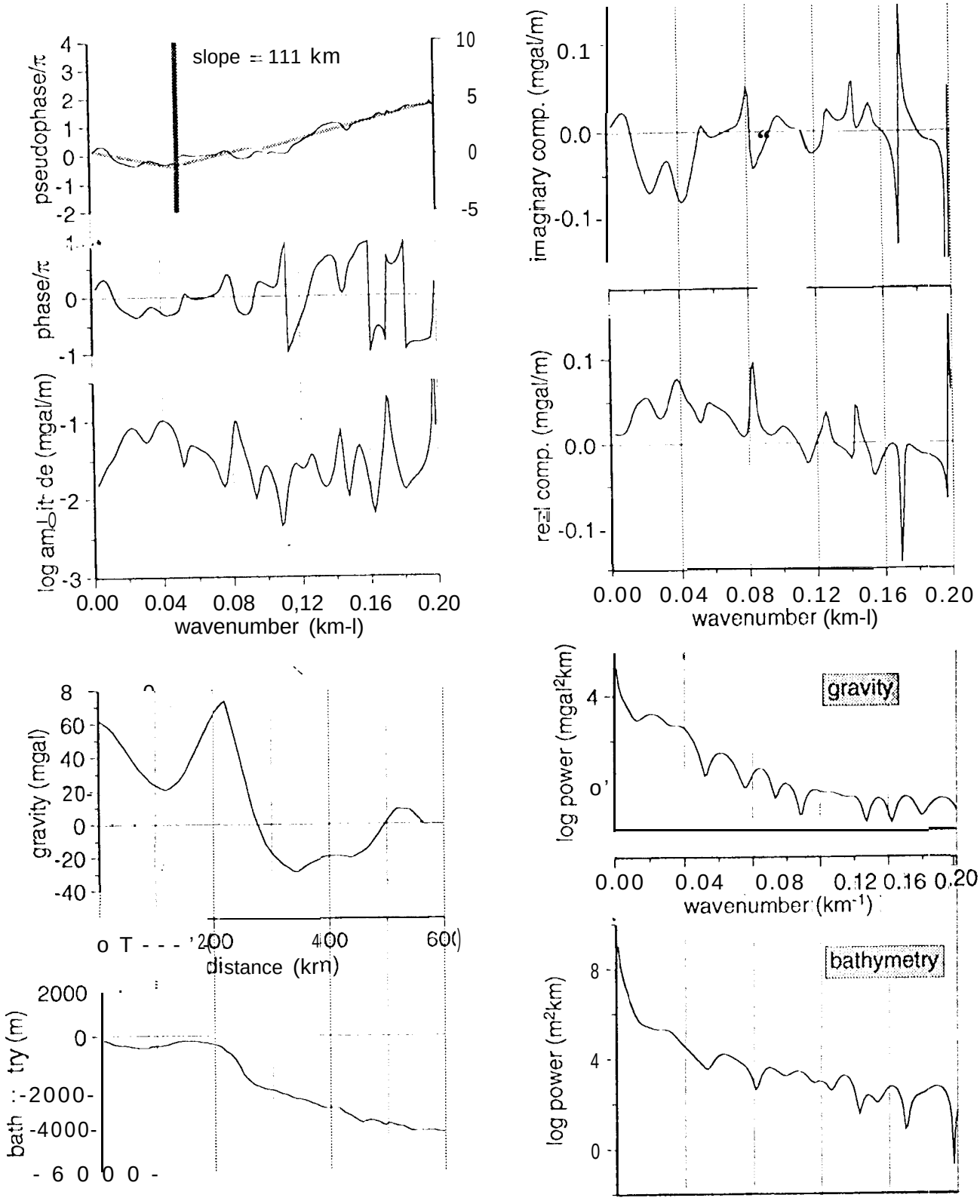

Figure A3. Admittance of a profile from 65°S latitude on the western Weddell margin.

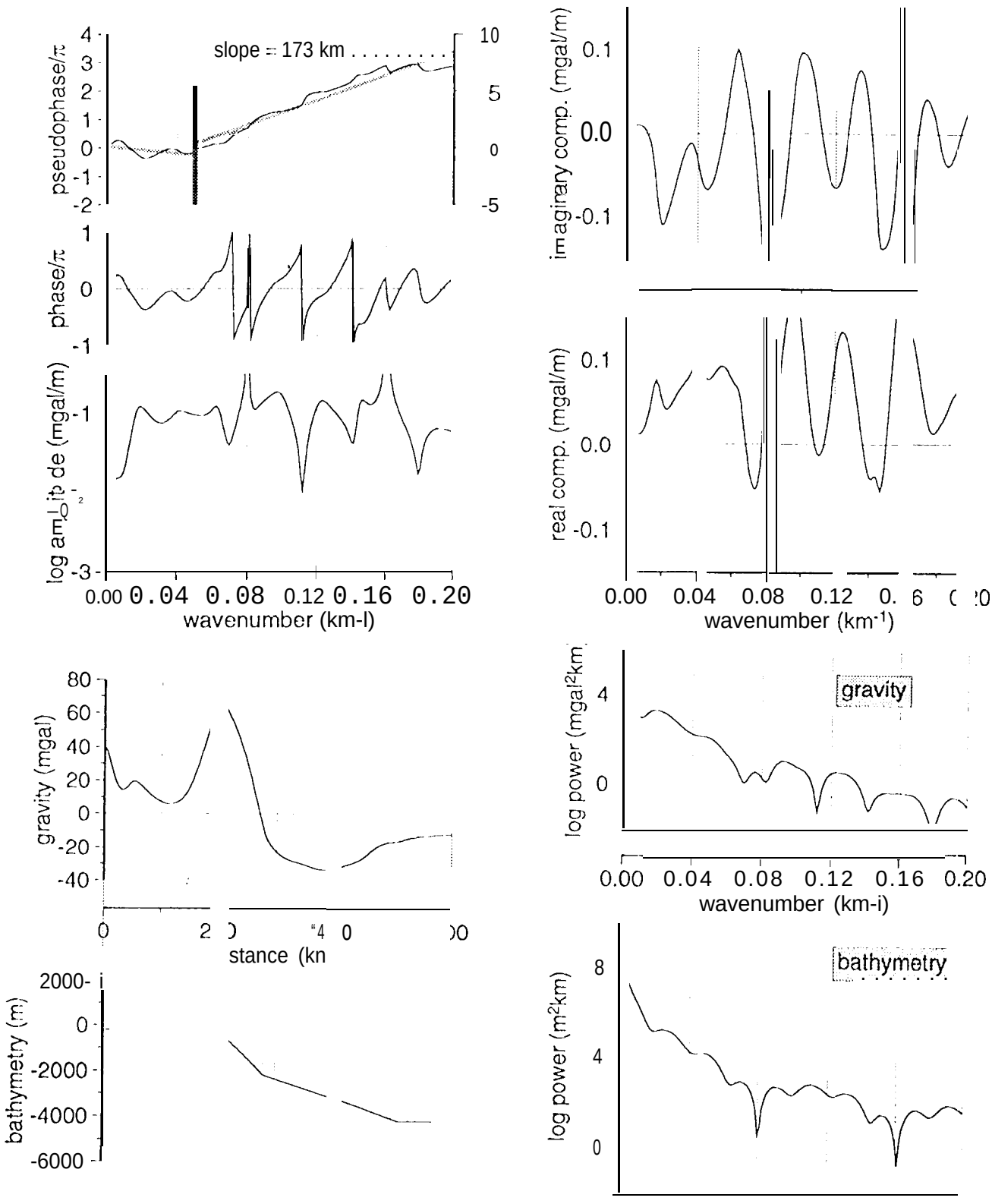

Figure A4. Admittance of a profile **modeled after** Figure A3 as described in the text in order to demonstrate the spectrum performance in the absence of noise.